Homogenous-Heterogenous reactions in the flow of pseudo-plastic nanofluid

Thesis submitted by

Syed Muhsin Abbas Naqvi

(01-248192-009)

Supervised By

Dr. Jafar Hasnain

Department of Computer Sciences

Bahria University Islamabad, Pakistan

Session (2019-2021)

Homogenous-Heterogenous reactions in the flow of pseudo-plastic nanofluid

Thesis submitted by

Syed Muhsin Abbas Naqvi

(01-248192-009)

Supervised By

Dr. Jafar Hasnain

A dissertation submitted to the Department of Computer Science, Bahria University Islamabad as a partial fulfillment of the requirement of the award of the degree of MS

Department of Computer Sciences

Bahria University Islamabad, Pakistan

Session (2019-2021)

Bahria University
Discovering Knowledge

MS-13

Thesis Completion Certificate

Student Name: **Syed Muhsin Abbas Naqvi** Registration Number**: 66196**

Program of study: **MS (Mathematics)**

Thesis Title: **"Homogenous-Heterogenous reactions in the flow of pseudo-plastic nanofluid''**

It is to certify that the above student's thesis has been completed to my satisfaction and to my belief, its standard is appropriate for submission for evaluation. I have also conducted plagiarism test of this thesis using HEC prescribed software and found similarity index at 18% that is within the permissible limit set by HEC for MS/MPhil degree thesis. I have also found the thesis in a format recognized by the Bahria University for MS/MPhil thesis.

Principal Supervisor's signature: _____ ____

Name: **Dr. Jafar Hasnain**

Date: _____

Bahria University
Discovering Knowledge

MS-14A

Author's Declaration

I, Syed Muhsin Abbas Naqvi, hereby state that my MS thesis Titled **"Homogenous-Heterogenous reactions in the flow of pseudoplastic nanofluid"** is my own work and has not been submitted previously by me for taking any degree from Bahria University or anywhere else in the country/world.

At any time if my statement is found to be incorrect even after my graduate, the university has the right to withdraw/cancel my MS degree.

Name of student: **Syed Muhsin Abbas Naqvi**

Date: _____

Bahria University
Discovering Knowledge

MS-14B

Plagiarism Undertaking

I, **Syed Muhsin Abbas Naqvi** solemnly declare that research work presented in the thesis titled **"Homogenous- Heterogenous reactions in the flow of pseudo-plastic nanofluid"** solely my research work with no significant contribution from any other person. Small contribution/help wherever taken has been duly acknowledge and that complete thesis has been written by me.

I understand the zero-tolerance policy of the HEC and Bahria University towards plagiarism. Therefore, I as an author of the above title thesis declare that no portion of my thesis has been plagiarized and any material used as reference is properly referred/cited.

I undertake that if I am found guilty of any formal plagiarism in the above titled thesis even after award of MS degree, the university reserves the right to withdraw/revoke my MS degree and that HEC and the University has the right to publish my name on the HEC/University website on which names of students are placed who submitted plagiarized thesis.

Author's sign: _____

Name of the Student: Syed Muhsin Abbas Naqvi

Dedication

I dedicate my thesis to my worthy parents because whatever I am, is due to my parent's hard work whose prays, love and endless sport have been a source of inspiration and encouragement for me.

I also dedicate this thesis to my respected supervisor Dr. Jafar Hasnain who has intellectually accompanied me in my research enquiry and impressed me by this hard work and sincerity.

Acknowledgements

Everlasting praise to **ALLAH Almighty** the most gracious, the most merciful who bestowed me with His great blessings. I am really blessed as He gave me the ability to think even upon a little tiny thing He created. He gave me a source (His beloved **PROPHET (PBUH)**) of light for my way to him. I would like to express my sincere gratitude to my kind mentor and supervisor Dr. Jafar Hasnain, associate professor Department of Computer Science, Bahria University, Islamabad for his persistent, continuous, dedicated, and pertinent guidance that kept me motivated to complete my thesis. It has been an honor to have him as my supervisor for my MS thesis. I express my sincere respect and gratitude to my all teachers who have given their valuable support cooperation and suggestion from time to time in my study.

My appreciation is to my family who always the real pillars of my encouragement showed their love, care and support throughout my life. As usual, so many friends and my classmates have helped me throughout my MS that I cannot list them all. Dr. Syed Saqib Shah, Nomana Abid, Tabinda Sajid, Ali Raza, Huda Chaudry, Zeeshan Zahoor, and Robash Qasim were specially remained enormously helpful throughout the period of my MS studies.

Syed Muhsin Abbas Naqvi

Bahria University Islamabad, Pakistan

November 2021.

Abstract

The purpose of the present study is investigating the heat transfer of non-Newtonian pseudo-plastic nanofluid flow on a moving permeable flat plate with viscous dissipation and heat absorption/generation. The flow is uniform and parallel to the moving flat plate, and both flat plate and flow are moving in the same directions. The investigated parameters in this study are power-law index, permeability parameter, Eckert number, volume fraction of nanoparticles, nanoparticles type, velocity ratio and heat absorption/generation parameter. The nanoparticles used in this paper are Al_2O_3, TiO_2, Cu and CuCo dispersed in the base water and sodium carboxymethyl cellulose/water as the base fluid. By using suitable transformations, the governing partial differential equations are converted into the ordinary differential equations, and after that, the resulting ODEs are solved with Runge–Kutta numerical method. The results of this investigation showed that heat transfer of Newtonian and non-Newtonian nanofluids in the presence of viscous dissipation and generation/absorption of heat has an interesting behavior: For Newtonian fluid, by increasing the amounts of high-conductive nanoparticles to carrying fluid, a higher heat transfer is not obtained. For instance, copper nanoparticles, despite having highest thermal conductivity compared to other nanoparticles, show the lowest local Nusselt number. However, for pseudo-plastic non-Newtonian nanofluids the reversed trend was observed. Furthermore, in both Newtonian and non-Newtonian nanofluids, the local Nusselt number decreased by increasing injection parameter, heat generation or volume fraction of nanoparticles. Also effect of chemical reaction within the PP nanofluid flow in the presence of magnetohydrodynamic, heat generation/absorption phenomena and generalized slip condition also considered.

Nomenclature

u, v	Velocity component along x, y direction
x	Co-ordinate along the plate
y	Co-ordinate to the plate normal to the plate
U	Composite velocity
U_w	Plate velocity
U_∞	Flow velocity
v_w	Mass transfer velocity
λ	Velocity ratio
Pr	Prandtl number
T	Temperature
T_∞	Outside the boundary layer temperature
T_w	Plate temperature
Ec	Eckert number
f_w	Suction/injection parameter
k	Thermal conductivity
f	Dimensionless stream function
Re_x	Local non-Newtonian Reynolds number
C_p	Specific heat at constant pressure
C_{fx}	Local skin friction coefficient
n	Power law index
Nu	Local Nusselt number
Sc	Schmidt number
K_s	Strength of heterogeneous reaction
K	Strength of homogeneous reaction
G	Dimensionless homogeneous function
H	Dimensionless heterogeneous function
K_c^*	Chemical species for A

K_s^*	Chemical species for B
D_A	Diffusion coefficient (homogeneous reaction)
D_B	Diffusion coefficient (heterogeneous reaction)
f_w	Suction/injection parameter
γ	Heat generation/absorption
Nu_x	Local nuslet number
C_{fx}	Local skin fraction number
IV P	initial value problem
BC	Boundary conditions
BL	Boundary layer
PW	Power law
HH	Homogeneous-Heterogeneous
PDE	Partial differential equation
ODE	Ordinary differential equation
R-K	Runge-Kutta
$f'(\eta)$	velocity profile
$\theta(\eta)$	temperature profile
SS	shear stress

Greek alphabet

η	Similarity variable
μ	Dynamics viscosity
θ	Dimensionless temperature
ν	Kinematics viscosity
δ	Diffusion coefficient of heterogeneous
ϕ	Nanoparticle volume fraction
γ	Local heat generation/absorption parameter
ψ	Stream function
ϵ	Slip parameter

Subscripts

f	Fluid
w	Condition at surface
nf	Nanofluid
s	Solid

List of Tables

List of figures

Chapter 1

Introduction

The purpose of this chapter is to emphasize on associated definitions and laws that describe the flow and heat transfer in non-Newtonian fluids over a permeable moving plate. The basic concepts and techniques for solving the governing equations.

1.1 Definitions and Preliminaries

1.1.1 Fluid

Fluid is a substance that has no fix shape and continually deforms under an applied external shear stress on it. It may be a liquid or gas. i.e., milk, honey, gasoline, and methane.

1.1.2 Nanofluid

It is the type of liquid that consists of the suspensions of nanoparticles in a base fluid. The term nanofluid refers to a fluid that contains nanometer sized particles. Nanotechnology has attracted the interest of researchers in recent years because of its huge economic revolution.

1.1.3 Flow

The material where unlimited deformation of the substance is increasing constantly.

1.1.4 Density

Mass per unit volume is said to be fluid density.

$$\rho = \lim_{\delta v \to 0} \left(\frac{\delta m}{\delta v} \right), \tag{1.1}$$

where δv is small volume enclosing a mass δm of the fluid.

1.1.5 Pressure

It is the amount of force that is applied vertical to the surface of an object per unit area all over force is distribute equally in all direction.

It is represented by $P^{\cdot}$. It can be mathematically written as

$$P^{\cdot} = \frac{F^{\cdot}}{A^{\cdot}}, \tag{1.2}$$

here $F^{\cdot}$ denotes force and $A^{\cdot}$ represents area.

1.1.6 Steady flow

In steady flow the velocity vectors and other fluid parameters (velocity, pressure, and cross-section of stream) at each place of fluid remain constant throughout time. It can be expressed mathematically as:

$$\frac{\partial \xi^*}{\partial t} = 0, \tag{1.3}$$

where ξ^* is any fluid Property

1.1.7 Unsteady flow

In unsteady flow is classified as unsteady if the fluid parameters (velocity, pressure, and cross-section of stream) change over time at any point in the fluid. It can be expressed mathematically as,

$$\frac{\partial \xi^*}{\partial t} \neq 0, \tag{1.4}$$

1.1.8 Laminar flow

In laminar flow each particle of fluid remains in its own path and does not cross one another or all particles moving in a particular path.

1.1.9 Porous medium

Porous media are those that have tiny openings in their surface that enable fluids to flow through them. Porous-surfaced items contain vacuum areas or pores by which fluid particles may pass. Wooden materials, sand, tissue papers, sponges and foams are examples of porous medium.

1.1.10 Slip flows

Slip flow is considered when the relative velocity is nonzero at surface and adjacent fluid particles. As stated, this case is rare in microfluidics. In various applications, slip boundary condition plays a vital role especially when the fluid is particulate, for instance, foam and polymer solutions, emulsion suspension, bubbles, etc.

1.1.11 No slip flows

In no-slip flow regime, the relative velocity of the liquid and wall is zero. At low pressure this condition does not hold.

1.1.12 Pseudo-plastic fluid

Pseudoplastic fluid is a fluid whose viscosity decreases as SS increases. It is a type of non-Newtonian fluid. Paint, honey and ketch-up are examples of pseudoplastic fluid.

Mathematically it can be expressed as

$$\tau_{xy} = k\left(\left|\frac{\partial u}{\partial y}\right|^{n-1}\left(\frac{\partial u}{\partial y}\right)\right), n < 1. \tag{1.5}$$

here k represents consistency index, n is flow behavior index.

1.1.13 Homogeneous reactions

When the chemical reaction occurs between same states of matter such as solid-solid, liquid to liquid, or gas to gas is known as homogeneous reaction. The combination is

observed in methane gas and oxygen to produce flame. Reactions among liquids or substances melt down in liquids.

$$\bar{\bar{A}} + 2\bar{\bar{B}} \rightarrow 3\bar{\bar{B}}, \quad rate = K_c^* ab^2, \tag{1.6}$$

1.1.14 Heterogenous reactions

When the chemical reaction occurs in more than one phase is known as heterogeneous reaction. For example, Solid and gas, solid and liquid. Heterogeneous reactions include those involving acids and metals, as well as those involving air and seawater.

$$\bar{\bar{A}} \rightarrow \bar{\bar{B}} \ , \quad rate = K_s^* a, \tag{1.7}$$

1.2 Basic Laws

1.2.1 Law of conservation of mass

This law states that the mass is neither established nor demolished in any isolated system. The mass of reactant is equal to the mass of product. Mathematically it can be expressed for compressible fluid as

$$\nabla \cdot \left(\rho \vec{V}\right) + \frac{\partial \rho}{\partial t} = 0 \ , \tag{1.6}$$

similarly, for incompressible fluid. (ρ is constant)

$$\nabla \cdot \vec{V} = 0. \tag{1.7}$$

1.2.2 Law of conservation of energy

This law state that total energy of isolated system neither produced nor destroyed throughout the whole procedure. But it can be converted another form i.e., potential to kinetic energy. Mathematically, it can be written as

$$E = T + V. \tag{1.8}$$

Similarly in case of law of conservation of momentum, momentum neither created nor destroyed.

1.2.3 Newton law of viscosity

This law declares that the relationship between shear stress varies directly to negative value of velocity gradient in middle of similar couple adjacent fluid's layers. Mathematically it can be written as,

$$\tau_{yx} = -\mu \frac{\partial u}{\partial y}, \tag{1.9}$$

where μ is dynamic viscosity.

1.2.4 Heat transfer modes

There are three common heat transfer modes as given below

(i) Convection
(ii) Conduction
(iii) Radiation

Convection

The procedure in which heat transfer takes place between objects by direct contact or heat transfer takes place within the fluid. For example, heat transfer between air and water.

Conduction

The procedure in which heat transfer from the hot to the cold body due to free electrons is known as heat transfer by conduction.

Radiation

The process in which heat is transferred through waves motion. Example of radiation is heat from the sun warm up to our face.

1.3 Solution Methodology

Any mechanism of the phenomenon is observed in the form of PDE, but it is not an easy task to tackle them. The present mathematical model is formed according to some specific assumptions. The similarity variables are often used to transform PDEs into ODEs. Some methods are designed to solve the governing equations either analytical or numerical. The R-K method is famous numerical technique to solve the existing problem. It is useful technique due to its accuracy.

1.4 Runge-Kutta Method

Several numerical approaches are available to solve ODE's using IVP. R-K method is one of the precise successful procedures which is widely famous as R-K method. Second-order initial value problem is commonly expressed as

$$\frac{d^2y}{dx^2} = f\left(x, y, \frac{dy}{dx}\right), \tag{1.10}$$

$$y(x_o) = y_o\,, \frac{dy}{dx}(x_o) = a\cdot, \tag{1.11}$$

For solving the problem, the similarity transformations are employed to convert the second order IVP into the system of 1st order IVP.

$$\frac{dy}{dx} = \omega = g\cdot(x, y, \omega), \tag{1.12}$$

$$\frac{d\omega}{dx} = f(x, y, \omega), \tag{1.13}$$

Initial conditions are

$$y(x_o) = y_o\,,\ \omega(x_o) = c, \tag{1.14}$$

For above system of 1st order differential equations (1.13 - 1.14) subject to BCs (1.15), the R-K method is given below

$$y_{n+1} = y_n + \frac{1}{6}(a_1 + a_2 + a_3 + a_4), \tag{1.15}$$

$$\omega_{n+1} = \omega_n + \frac{1}{6}(b_1 + b_2 + b_3 + b_4), \tag{1.16}$$

where, $$a_1 = hg(x_n, y_n, \omega_n), b_1 = hf(x_n, y_n, \omega_n), \tag{1.17}$$

$$a_2 = hg\left(x_n + \frac{h}{2}, y_n + \frac{a_1}{2}, \omega_n + \frac{b_1}{2}\right), b_2 = hf\left(x_n + \frac{h}{2}, y_n + \frac{a_1}{2}, \omega_n + \frac{b_1}{2}\right), \tag{1.18}$$

$$a_3 = hg\left(x_n + \frac{h}{2}, y_n + \frac{a_2}{2}, \omega_n + \frac{b_2}{2}\right), b_3 = hf\left(x_n + \frac{h}{2}, y_n + \frac{a_2}{2}, \omega_n + \frac{b_2}{2}\right), \tag{1.19}$$

$$a_4 = hg(x_n + h, y_n + a_3, \omega_n + a_3), b_4 = hf(x_n + h, y_n + b_3, \omega_n + b_3), \tag{1.20}$$

Where the step size is uniform as,

$$h = \frac{x_n - x_o}{n}, \tag{1.21}$$

here n is the total steps.

1.5 Shooting Method

One of the numerical techniques used to solve BVP by reducing it into IVP. It is an iterative technique that is famous for the two-point boundary value problem. Then our aim is to sort out IVP instead of given BVP directly. We use R-K 4 after obtaining IVP.

Let us consider a boundary value problem

$$\frac{d^2y}{dx^2} = f\left(x, y, \frac{dy}{dx}\right), \tag{1.22}$$

with boundary condition are

$$y(0) = 0\,,\ y(L_1) = b, \tag{1.23}$$

Where f is by function $x = 0$ and $y = L_1$ the same differential equation describes as

$$y(0) = 0\,,\ y'(0) = p, \tag{1.24}$$

We convert PDE's into system of 1st order differential equations for solving BVP as,

$$\frac{dy}{dx} = u \, , \frac{du}{dx} = \ f(x, y. u), \tag{1.25}$$

with the initial condition,

$$y(0) = \ 0 \, , \ y'(0) = u(0) = p, \tag{1.26}$$

where s represents the missing initial condition which will be considered as initial value, after that we will be able to find the value of s using the initial condition (1.27) which satisfies the boundary conditions (1.24). If solution of initial value problem is represented by $y = (x, p) \; and \; u = (x, p)$ then to calculate the values of p , we suppose

$$y(L_1, p) - A = \ 0 = \phi(p). \tag{1.27}$$

With the help of Newton Raphson mothed we can solve the system of equations numerically by using the same guess given in equation (1.27) as

$$p^{n+1} = p^n - \frac{\phi(p^n)}{\frac{d\phi}{dp(p^n)}}, \tag{1.28}$$

$$p^{n+1} = p^n - \frac{\phi(L_1 \, , p^n) - A}{\frac{d\phi}{dp(L_1 \, , p^n)}}. \tag{1.29}$$

Differentiating y w.r.t the equation (1.26) and (1.27), we get

$$\frac{dY}{dx} = U \, , \frac{dU}{dx} = \frac{\partial f}{\partial u} Y + \frac{\partial f}{\partial u} U \, , \tag{1.30}$$

hence,

$$Y = \frac{\partial y}{\partial p} \, , U = \frac{\partial u}{\partial p}, \tag{1.31}$$

and the resulting initial value problem will be

$$Y(0) = 0 \, , U(0) = 1, \tag{1.32}$$

Solution of equation (1.22) satisfies the boundary conditions (1.23). We can get solution with the help of following steps given below,

(i) Denote s initial guess which is taken as a missing condition (1.26).

(ii) Solve the system equations (1.25) subject to initial conditions $x = 0\ and\ x = L_1$

(iii) The system of equations (1.30) integrated, according to initial conditions (1.32) from $x = 0\ and\ x = L_1$.

(iv) By using the value $Y\left(L_1, p^{(1)}\right) - A_1$ from step (ii) and $Y(L_1, p^1)$ obtain from step (iii) in the equation (1.29).

$$p^2 = p^1 - \frac{Y\left(L_1, p^1\right) - A}{Y(L_1, p^1)}, \tag{1.34}$$

Similarly, 2nd missing initial condition is p^2 obtained (v) Repeat all these steps (i) to (iv) until it shows value which specifies exponent accuracy $Y(L_1, p^2)$ which satisfied BCs of Eq (1.22).

Chapter 2

Literature review

2.1 Overview

In this chapter we have represented the study related to non-Newtonian fluid, MHD, generalized slips conditions, mass transfer with chemical reaction**.**

2.2 Related work

Fluid has vital role in engineering and technologies due to its importance and influences in the industrial field. The term nanofluid refers to a fluid that contains nano-sized particles. Because of its huge economic revolution, revolutionary nanotechnology has attracted the interest of researchers in the recent years. Computational tools combined with a research laboratory framework have provided additional insight into fluid flow problems in recent years. The fluids industry is becoming to increasingly interested in the field non-Newtonian. Because of the numerous applications the heat transfer in various industries, enhancing the efficiency of thermal devices is currently one of the top concerns for industrial unit for designers. Improvements in temperature efficiency and increasing the efficiency of thermal devices saves energy. Reducing space and, as a result, reducing the size of gadgets minimize the device's material and production costs.

Nanotechnology advancements during the last two decades, as well as the use of nanofluid an exceptional medium for heat transmission, have launched latest frontiers for researchers. When compared to solids with metallic bases, the common heat transmission fluids in the engineering, like H_2o and $C_2H_6O_2$ has lowest heat conduction. Revolutionary nanotechnology has piqued academics' interest in recent years because of its massive economic revolution. Maleki *et al.* [1] examine the thermal transformation of pseudo-plastic nanofluid flow on moving porous flat plate with viscous dissipation and thermal generation/absorption in BL. CMC/H_2O was taken as a basic fluid with the nanoparticles

of $Al_2O_3, TiO_2\ Cu$ and CuO. Summary of problem is stated that pseudo-plastic nanofluids have ultimate thermal performance, related with Newtonian nanofluid. However, inclining in drag friction factor values for non-Newtonian nanofluids case become too small, while compare it with Newtonian nanofluids. Amin [2] worked on fluid flow with heat transfer in vibrating lid-driven cavity that is full by CuO/water nanofluid as well as current non-Newtonian conduct. The result given that, Boosting *Ha* number causes Nu to reduce in several volume fractions, Wo and PLI. By inclining in PLI will start to Nu reduce in several volume fractions and Wo numbers. Javad *et al.* [3] researched on extract exact solutions of power law model time dependent nanofluid in the presence of heat. To determine the physical conduct of nanofluid for shear thinning with shear thickening fluids, outcomes was gained distinctly for every circumstance. Impact of physicals parameter including volume fraction of nanoparticles, permeable, injection/ suction, and temperature radiation on flow and heat transfer of fluid debates was done one by one. Ali *et al.* [4] examine BL flow and heat transfer of non-Newtonian PLI fluid passed via an exponential stretched sheet with power-law slip condition in existence of an intensive magnetic field including Thermal radiation and hall current was considered. Major findings are, the Both thermal BL thickness and momentum are considered to decreased quicker for pseudo-plastic as compared to dilatant fluid. The temperature profile is enhanced as soon as magnetic variable, thermal radiation and PLI are enlarged. Gopal *et al.* [5] researched on the problematic of two dimensional, steady, laminar flow of a power-law fluid passing through a moving flat plate under the effect of perpendicular magnetic field. Conclusion is that the impact of magnetic field variable M is to decrease velocity parameter reversable phenomenon is observed closed to the plate.

Khan *et al.* [6] observed channel flow of nanofluids in a porous wall as well as permeable medium. Major opinion of his study was to be investigating the behavior of porosity walls on momentum and thermal transfer. The properties of several parameters, like thermal volume fraction, Grashof number, many kinds of nanoparticles, magnetic, radiation, suction/injection, permeability are observed in many types of plots. Velocity of Ag nanofluids reduces as enhancing the magnetic profile on the other hand deny the conduct which is examined in situation of injection. they conclude the result for various

kinds of nanoparticles which has many impacts on temperature and velocity profile because of suction and injection. Khan *et al***.** [7] were observed when velocity of nanofluids rises by inclining of volume fraction, permeability, and radiation variable in circumstance of suction however a reverse conducts was found in situation of injection. Velocity of Ag nanofluids reduces by inclining of magnetic parameter whereas disagreeing behavior is observed in injection case. temperature of Ag nanofluids was determined to reduce by inclining of φ for the extraction of fluid from the walls although too minor changes are noted during the stations of injection and conclude the results for various nanoparticles have various impacts on the velocity and temperature due to suction/injection. Waleed *at al.*[8] examine geographies of heat transfer in stagnation point flow about variable thickened surface. The main studies are manufactured as, velocity profile has a opposite behavior for first order and second-order slip parameters. The conduct is same for n on temperature parameter and velocity, but differing condition was noted due to Ha for temperature and velocity parameters. Ejaz *et al.* [9] discussed Tiwari Das model for effect of a magnetic field on non-Newtonian nanofluid flow in existence of injection and suction, investigate Blasius flow. consider the causes for magnetic field with a power law index. Furthermore, Newtonian, and non-Newtonian condition for Blasius flow is assumed. The impact of various parameters on temperature and velocity parameter for Blasius is discussed. They considered some valuable outcomes from which are follows as velocity reduce for Blasius flow versus different values of volume fraction for Newtonian and non-Newtonian fluid cases. In both cases of fluid, the Blasius flow decline with respect to velocity parameter to decreasing the value of transpiration rate. Thermal parameters are observed expansion of Blasius flow case verses increasing volume fraction in Newtonian fluid, Thermal profile inclining by enhancement in the Prandtl number. Jabeen *at al.* [10] worked on the steady flow of the viscous incompressible Newtonian fluid having a magnetic field with porous impact is examined that velocity profile decline by enlarging the magnetic parameter (M), although opposite impacts are noted in station of temperature and concentration profiles. Thermal profile and concentration declining with the value of Pr and Sc, respectively. Thermal BL thickness become enlarges by inclining of Ec and R values respectively. The concentration profile becomes greater by boosting the value of Sc. under viscous dissipation and ohmic dissipation.

Sajid *et al.* [11] was investigated the heat and mass transfer in MHD mixed convectional nanofluid flow on a time dependent stretched sheet. CMC/H_2O was considered as carrier fluid with diverse kinds of nanoparticles. The nanoparticles impact tends to, higher temperature of TiO_2-water nanofluid then the other nanofluids. Mass flux enlarged by inclining the nanoparticles, whereas greater Solute concentration of Al_2O_3-water nanofluid then the other nanofluids. Srinivasacharya *et al* [12] worked on Hall effect on viscous incompressible fluid flow over an exponentially stretchable sheet. They also examined the Suction-injection parameters, velocity slip and Joule heating effects. The discoveries was finalize when magnetic parameter inclining, the tangential velocity and heat and mass transfer rate decline[13] but the cross flow velocity, thermal profile and concentration inclining M. Alarifi *et al*. [14] consider steady laminar flow over a perpendicularly stretched sheet in the presence of viscous dissipation, heat source/sink, and magnetic fields. The Nu_x at the sheet surface augments, because the Hartmann number (Ha), stretching velocity ratio A, and mixed convection profile λ incline. However, it reduces and depend on co-efficient of heat generation/absorption. Malik *et al.*[15] examine the influence of HH reactions in Williamson fluid model with heat transfer phenomenon over a stretching cylinder. The major discovery of problem is specified that the Velocity and thermal profile inclining by enhancing in the curvature profile K. Velocity decline. when raises the strength of HH reaction L and Ls the concentration profile decline Skin friction is greater for bigger values of K although declining by raising Weissenberg number λ. Rate of heat transfer rises for greater all value of K and Pr. Prathap Kumar *et al.* [16] focus on problematic of solute dispersion of a solute for compound porosity medium concerning with dual parallel plate in the existence of first-order HH chemical reactions Effective dispersion coefficient and volumetric flow rate was found for thrice kind of boundary conditions. Name as insulating, insulating porous and permeable-insulating wall conditions for homogeneous chemical reaction also for combined outcome for HH chemical reactions. Outcomes gained for homogeneous permeable-impermeable wall boundary conditions have effective dispersion coefficient reduces as the viscosity ratio and pressure gradient inclining although it raises as the porous parameter inclining.

Hayat *et al.* [17] examined HH reactions special effects in BL flow of nanofluids flow over a nonlinear stretching sheet with variable thickness was examined. Flow was prevalent in kerosine and engine oils while compare with the water nanofluid. Abbas *et al.* [18] analyzed the numerical forms of the stagnation point flow of nanofluid in the presence of a magnetic field. The TD model is considered to generate equations of the flow problem with Thompson and Troian slip conditions. Mass transfer as well as heat transfer analysis was discussed with both HH reactions cases. They also explored conclusion for two types of slip condition (generalized slip and partial slip). The generalized slip and partial slip boundary conditions indicates that there is a prominently variations into velocity profiles due to generalized slip boundary conditions for both types of nanofluids. Kameswaran *et al.*[19] also HH reactions in a nanofluid flow due to a porosity stretched sheet Outcome was examined that concentration at the surface declining with the strength of the heterogeneous reaction for Cu and Ag–water nanofluids. Khan *et al*. [20] focus on study of MHD stagnation point flow of Casson fluid with regard to stretched out sheet. HH reactions jointly with homogeneous heat effect subjected to a resistive force of electromagnetic source was observed. They examine the chemical analysis and observe that Velocity field reduces the behavior for larger magnetic parameter. Kumar *et al.* [21] researched on challenge of solute dispersion of a solute for pair porous medium in the middle of couple parallel plates by the existence of 1^{st} -order HH chemical reaction. Impact of porosity parameter for soil, grains and wire cramps were decline in concentration which is same as outcomes gained through an experiment by Harleman et al. 1963.

Chapter 3

Effect of heat source/sink and viscous dissipation on pseudo-plastic nano liquid flow past a spongy stretching surface

3.1 Overview

In this chapter we Effect of heat source/sink and viscous dissipation on pseudo-plastic nano liquid flow past a spongy stretching surface. Let us take into the account steady BL flow in two dimensions. The governing dimensional equations in the case of flow model are transformed into system of non-dimensional ODE by utilizing suitable transformation. Numerically this system of equation is solved by utilizing shooting method along with R-K method. Basically, this chapter is review of Malaki *et al.* [1].

.

3.2 Mathematical Analysis

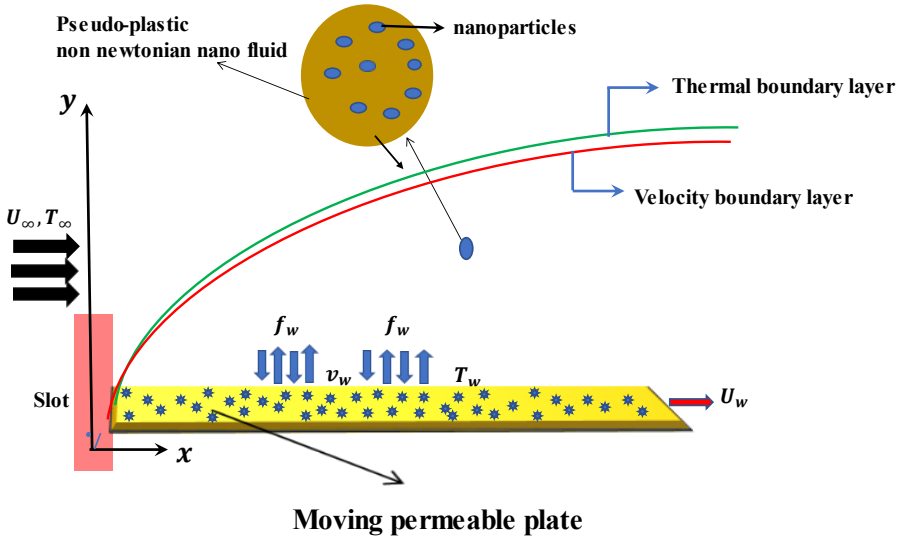

Figure 3.1

The graphical model and the co-ordinate system are presented in the fig. The plate and fluid move in same direction and NFs with CMC/H_2O having free stream velocity and temperature. CMC/H_2O had been utilized as a base fluid for a pseudo-plastic NN fluid. w component becomes zero due to BL. The governing equations for flow model will be in 2D because z component become zero. So, Pressure term also become because due to the BCs. The governing equations for flow model in form of continuity, Momentum and energy that can be express as,

$$\frac{\partial u}{\partial x}+\frac{\partial v}{\partial y}=0, \tag{3.1}$$

$$u\frac{\partial u}{\partial x}+v\frac{\partial u}{\partial y}=\frac{\mu_{nf}}{\rho_{nf}}\frac{\partial}{\partial y}\left(\left|\frac{\partial u}{\partial y}\right|^{n-1}\frac{\partial u}{\partial y}\right), \tag{3.2}$$

$$\frac{\partial T}{\partial x}+\frac{\partial T}{\partial y}=\alpha_{nf}\frac{\partial^2 x}{\partial y^2}+\frac{\mu_{nf}}{(\rho C_p)_{nf}}\left|\frac{\partial u}{\partial y}\right|^{n+1}+\frac{Q_o(T-T_\infty)}{(\rho C_p)_{nf}}, \tag{3.3}$$

Using following BCs which are given below,

$$\left.\begin{array}{c} u=U_w,\ \ v=-v_w,\ T=T_w \quad at\ \ y=0 \\ u\to U_\infty,\ \ T\to T_\infty \quad at\ \ y\to\infty \end{array}\right\}, \tag{3.4}$$

Here u and v are the velocity component along x and y direction while n is power law index of base fluid. u_w and u_∞ are plate and fluid velocity respectively.

Some useful similarity transformations are given below:

$$u=Uf'(\eta), v=\frac{y\,U}{x(n+1)}f'(\eta)-f(\eta)\frac{(U^{2n-1}\nu_f)^{\frac{1}{n+1}}}{(n+1)(x)^{\frac{n}{n+1}}},\ \eta=y\left(\frac{U^{2-n}}{\nu_f x}\right)^{\frac{1}{n+1}}, \tag{3.5}$$

Equation (3.2) and (3.3) are transformed as,

$$m_o(|f''|^{n+1}f'')'+\frac{1}{n+1}f''f=0, \tag{3.4}$$

$$\theta''+\frac{P_r m_1}{(n+1)}f\theta+\ \ P_r m_1 m_2 E_c|f''|^{n+1}+P_r m_1 m_3\gamma\theta=0. \tag{3.5}$$

Boundary conditions are,

$$\left.\begin{array}{c} f' = \lambda,\ \ f = f_w,\ \theta = 1 \text{ at } \eta = 0 \\ \mathrm{f}' \to 1 - \lambda,\ \ f = f_w,\ \theta \to 0 \text{ at } \eta \to \infty \end{array}\right\}. \tag{3.6}$$

Equation (3.10) and (3.11) have some parameters which can be express as,

$$P_r = \frac{U}{\alpha_f x}\left(\frac{U^2 - n}{\nu_f x}\right)^{\frac{-2}{n+1}}, E_c = \frac{U^2}{(C_P)_f\,(T_w - T_\infty)}\ ,\quad \gamma = \frac{Q_o x}{U\,(T_w - T_\infty)(C_P)_f},$$

$$\mu_{nf} = \frac{\mu_f}{(1-\varphi)^{2.5}}, \qquad \frac{k_{nf}}{k_f} = \frac{(k_s + 2k_f) - 2\varphi(k_f - k_s)}{(k_s + 2k_f) + \varphi(k_f - k_s)}, \qquad \alpha_{nf} = \frac{k_{nf}}{(\rho C_p)_{nf}},$$

$$\mu_{nf} = \frac{\mu_f}{(1-\varphi)^{2.5}}\ ,\quad f_w = (n+1)\left(\frac{x^n}{\nu_f U^{2n-1}}\right)^{\frac{1}{n+1}}\nu_w,\ \ Re_x = \frac{U^{2-n}x^n}{\nu_f}.$$

Engineering quantities can be written as,

$$m_o = \frac{1}{(1-\phi)^{2.5}\left[(1-\phi) + \phi\frac{\rho_s}{\rho_f}\right]}, \qquad m_1 = \frac{\left[(1-\phi) + \phi\frac{(\rho C_p)_s}{(\rho C_p)_f}\right]\left[\left(\frac{k_s}{k_f} + 2\right) + \phi\left(1 - \frac{k_s}{k_f}\right)\right]}{\left[\left(\frac{k_s}{k_f} + 2\right) - 2\phi\left(1 - \frac{k_s}{k_f}\right)\right]},$$

$$m_2 = \frac{1}{\left[(1-\phi)^{2.5} + \frac{\phi(\rho C_p)_s}{(\rho C_p)_f}\right]}\ , m_3 = \frac{1}{\left[(1-\phi) + \frac{\phi(\rho C_p)_s}{(\rho C_p)_f}\right]},$$

$$\lambda = \frac{U_w}{W_\infty}.$$

In above terms m_o, m_1 and m_2 are nanofluid constant, λ is velocity ratio, U_w and U_∞ is plate and fluid velocity. $U = U_w + W_\infty$, where U is composite velocity signified by Afzal *et al.* [23]. At condition $0 < \lambda < 1$ is related to the state that fluid and surface are moving in similar path. At $\lambda < 0$ and $\lambda > 0$ state that both are moving in opposing path. When $\lambda = 1$ flat plate moves, and fluids remains in rest. When $\lambda = 0$ the plate is fixed, and fluid is in motion. Our focus is on the condition of $0 \le \lambda \le 1$. (Nu_x) and (C_{fx}) can be written as,

$$C_{fx} = -\frac{2\tau_w}{\rho_f U^2}\ , Nu_x = \frac{x q_w}{k_f(T_w - T_\infty)}. \tag{3.9}$$

The surface thermal flux (q_w) and surface shear stress (τ_w) calculated as,

$$\tau_w = \mu_{nf}\left(\left|\frac{\partial u}{\partial y}\right|^{n-1}\frac{\partial u}{\partial y}\right)_{y=0}, q_w = -k_{nf}\left(\frac{\partial T}{\partial y}\right)_{y=0}. \tag{3.10}$$

Applying similarity parameters (3.5) obtained equations are

$$\frac{1}{2}C_{fx}Re_x^{\frac{1}{n+1}} = -m_4\, f''(0)|f''(0)|^{n-1}\ , Nu_x Re_x^{\frac{-1}{n+1}} = m_5\,\theta'(0), \tag{3.11}$$

3.2.1 Solution methodology

The governing nonlinear differential equations (3.4) and (3.5) with boundary conditions of Equations (3.6) are tackled numerically by using R-K method and the shooting algorithm is applied to solve the nonlinear BVP. This approach is entirely achieving outstanding accuracy. This method has also been applied successfully in many non-Newtonian fluid flow problems in recent years because it converges rapidly and provides batter accuracy. From equations (3.4) -(3.5) convert the ordinary differential equation as,

$$y_1^* = f, y_2 = f', y_3 = f'', y_3' = f''',\ y_4 = \theta,\ y_5 = \theta',\ y_5' = \theta'', \tag{3.14}$$

$$y_3' = -\frac{y_3 y_1^* |y_3|}{m_o(n-1)[(n-1)y_3|y_3|^{(n-2)}+|y_3||y_3|^{(n-1)}}, \tag{3.15}$$

$$y_5' = -\frac{P_r m_1}{(n+1)}y_1^* y_5 - P_r m_1 m_2 E_c|y_3|^{n+1} - P_r m_1 m_3 \gamma\, y_4. \tag{3.16}$$

Subject to boundary conditions

$$\left.\begin{aligned} y_1(0) = f_w, y_2(0) = \lambda, y_3(0) = s_1,\ y_4(0) = 1 \\ y_2(\infty) \to 1-\lambda,\ \ y_4(\infty) \to 0 \end{aligned}\right\}, \tag{3.17}$$

Table 3.1: Viscosity characteristics of CMC/H_2o base fluid with the help of [24]

Physical Properties	CMC/H_2O 0%	CMC/H_2O 0.1%	CMC/H_2O 0.2%	CMC/H_2O 0.3%
N	1	0.91	0.85	0.81
K/Ns^nm^{-2}	0.00085	0.00632	0.0175	0.0314

Table 3.2 :Thermophysical properties of CMC/H_2o and nanoparticle with the help of [25]

Physical properties	CMC/H_2o 0.0-0.3%	Cu	Al_2O_3	CuO	TiO_2
$C_p/Jg^{-1}K$	4179	385	765	553.6	686.2
ρ/kgm^{-3}	997.1	8933	3970	6500	4250
$k/Wm^{-1}K$	0.613	400	40	20	8.954

3.2.2 Outcomes and Discussion

The governing equations are solved numerically by applying R-K method and represented by graphically. We deeply observe effect which are take place on velocity and temperature profile by variating the different parameters. Impact of different parameters are shown in Figures. Figure (3.2) indicates the impact of f_w sucking/injection parameter on velocity profile. Suction/injection parameter stabilized the BL magnitude. By decreasing suction/injection parameter velocity profile also decreased gradually.

Figure (3.3) represent the effect of ϕ on both of velocity and temperature gradient. It is observed that by inclining ϕ heat and velocity are reduced. Although, temperature raised in the BL. By seeing the physical viewpoint, these higher values of nanoparticles cause the thermal BL thickness increased and the velocity BL thickness reduced. And by ϕ of nanoparticles increasing, the surface temperature gradient is diminishing. From Figures (3.4) elaborate the impression of power-law index n and Prandtl number on the velocity by giving the different values of n (power law index) doesn't keep any prominent effect on velocity. Graph is decreasing by increasing the value of power law index (n).

Figures (3.5) show the effect on velocity profile. In (3.5) the obtain outcomes are λ is in the range of 0 to 0.4 flow velocity is greater than plat velocity but when its range is 0.6 to 1 then plate have greater velocity as compared to free flow velocity. Lastly, when λ have value is 0.5 then observed velocity is same for flow and plat velocity and observed to be constant at every point. In figure (3.6) the graph is decreasing by increasing the volume fraction. Velocity profile is decreasing by increasing the volume fraction. Figure (3.7) signifies the impact of suction/injection parameter f_w on the heat and velocity profile. Suction/injection parameter stabilized the BL magnitude. By decreasing suction/injection parameter the heat profile is decreasing gradually. From discussion it's clear that at higher value of f_w (suction/injection) thermal gradient behavior closes the wall raises as compared to far away the wall and heat transfers also indicating from fluid to the surface.

Figure 3.8 shows the physical expressions on thermal profile by generation/absorption parameter. It's seen that by increasing $\gamma < 0$, temperature reduces, while temperature increased when γ is nonnegative. These physical phenomena declare that temperature

doesn't affects and lying on the wall but close the boundary layer. Boundary layer become thinner while enhancing the temperature absorbate generation. Figure (3.9) elaborate the impression of power-law index (n) and Prandtl number on temperature profile. Bestowing to the fig (3.9) by reducing n and rise in Pr number the temperature will reduce.

Figure (3.10) tells us the distribution of temperature for distinct values of Ec numbers. In relating along with no-viscous dissipation, enhancing the Ec which causes to increment in the temperature. Also, because of viscous heating, the expansion of fluid temperature turns out to be more momentous when Ec number is increasing. It should be noted that at the highest Ec numbers (Ec = 0.5), thermal transfer has a different behavior, with a different temperature gradient slope, heat transfers from the plate surface into the fluid, and a temperature increase in the interior of the BL, near the wall.

From figure (3.11) shows when swelling the velocity ratio λ,the temperature will reduce its means by rising velocity of plate, the thickness of temperature in BL does not increase. From fig (3.12) it clear that, the effect of utilizing various nanoparticles on local friction factor for Newtonian as well as non-Newtonian nanofluids cases. As observed from figure, in case of Newtonian as well as pseudo-plastic states, drag force is increasing by enhancement of ϕ . From fig values of skin friction factors highest or lowest depend on cu - and Al_2O_3-based nanofluids, correspondingly.

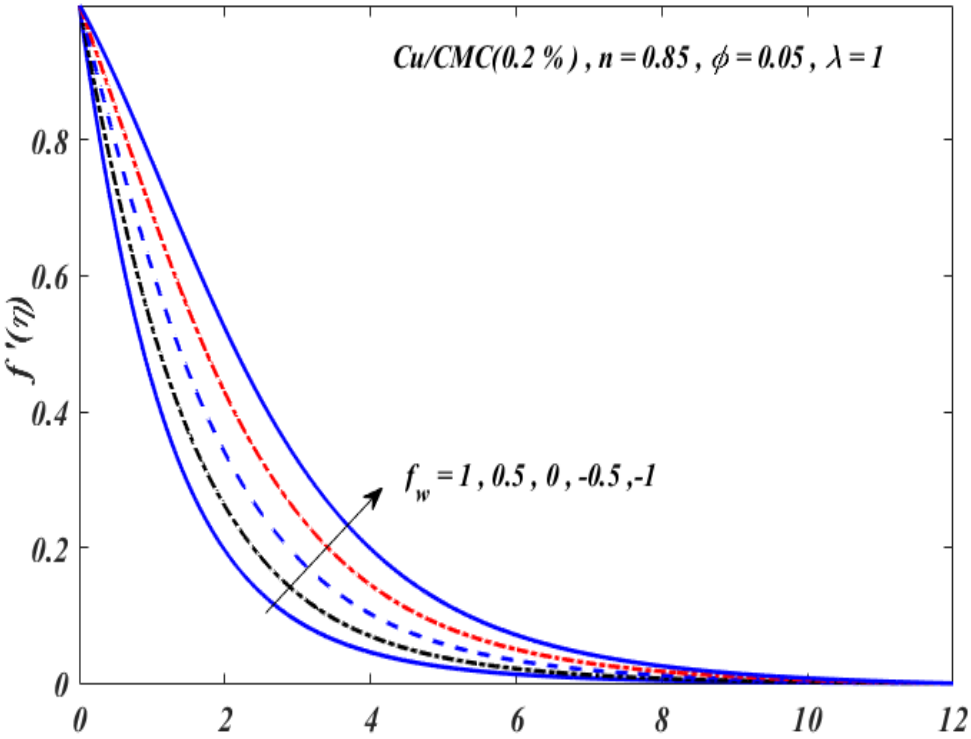

Figure 3.2: Porosity (suction) f_w on velocity profile $f'(\eta)$

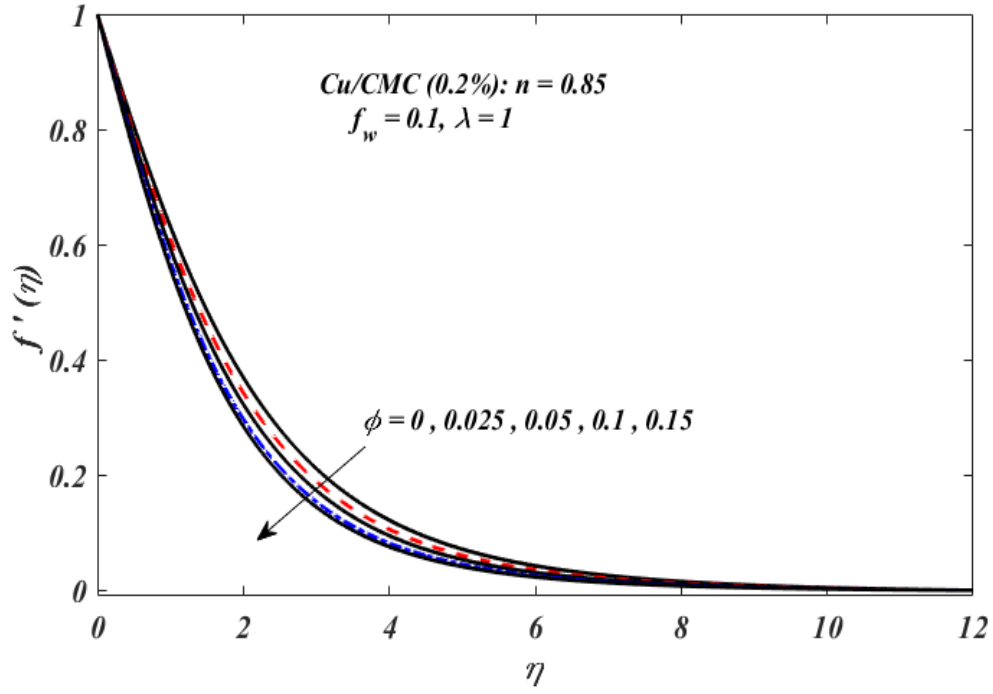

Figure 3.3: Effect of volume fraction ϕ on velocity profile $f'(\eta)$

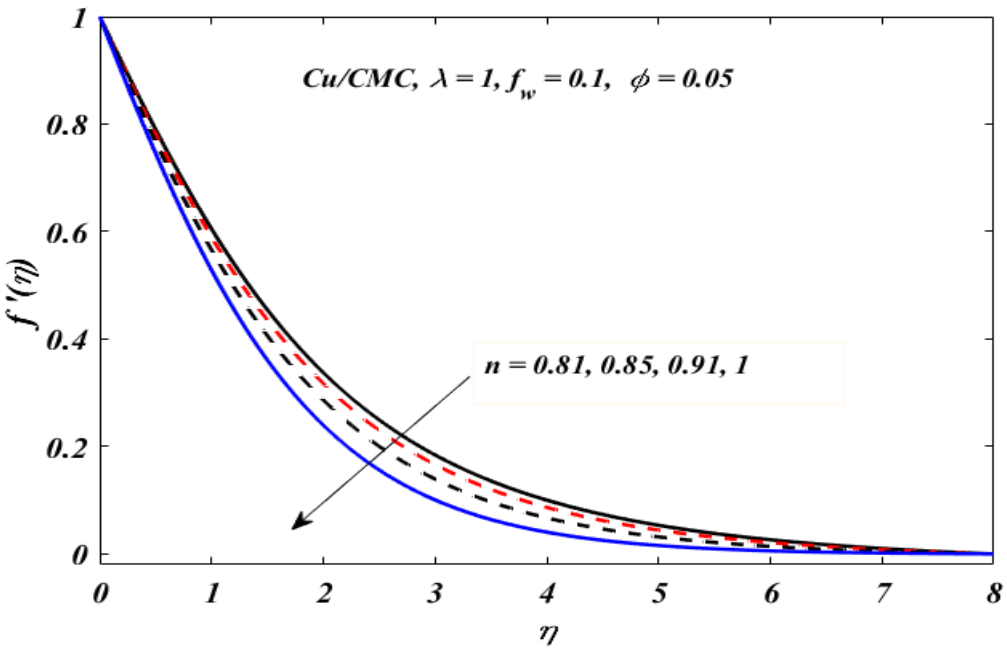

Figure 3.4: Effect of power law index n on velocity profile $f'(\eta)$.

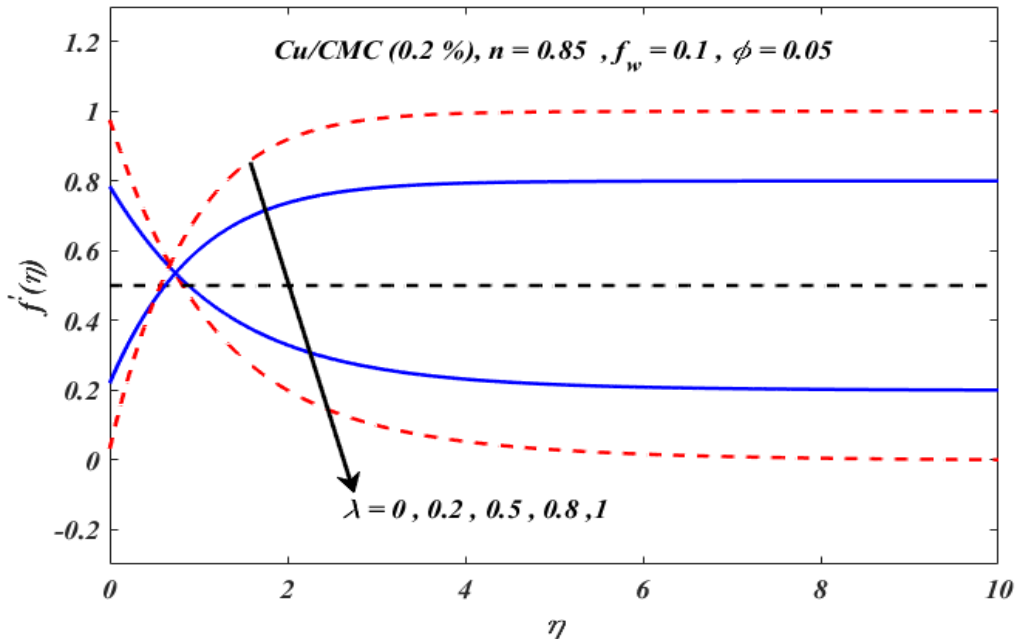

Figure 3.5: Effect of velocity ratio λ on velocity profile $f'(\eta)$.

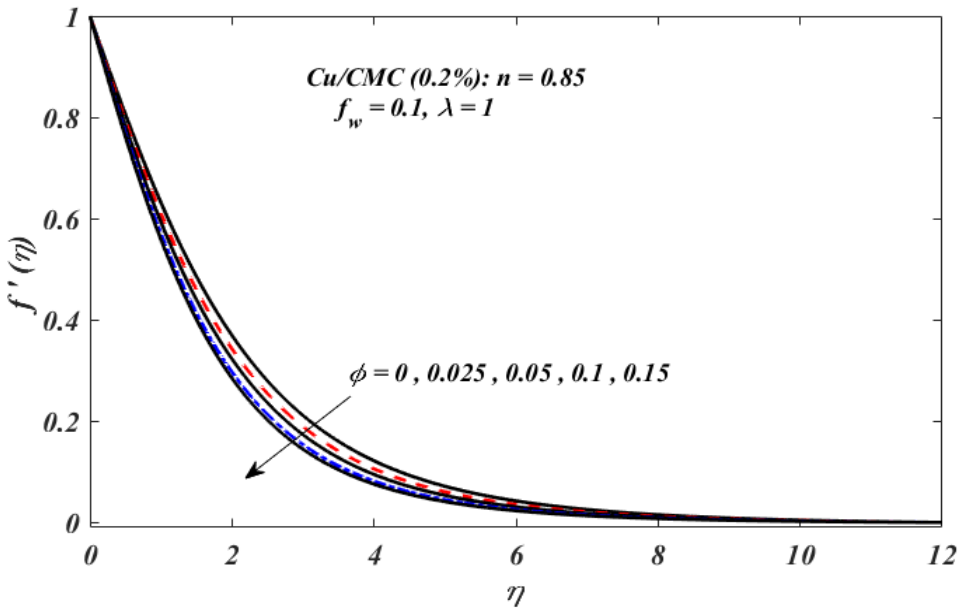

Figure 3.6: Effect of porosity (suction/injection) f_w on temperature profile.

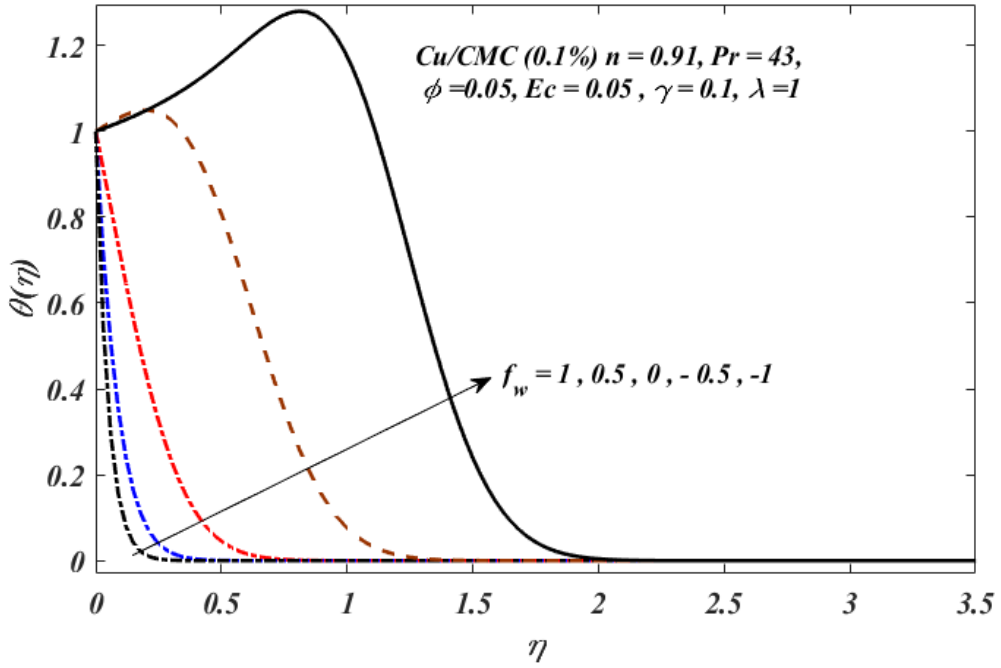

Figure 3.7: Effect of volume fraction ϕ on temperature profile $\theta(\eta)$.

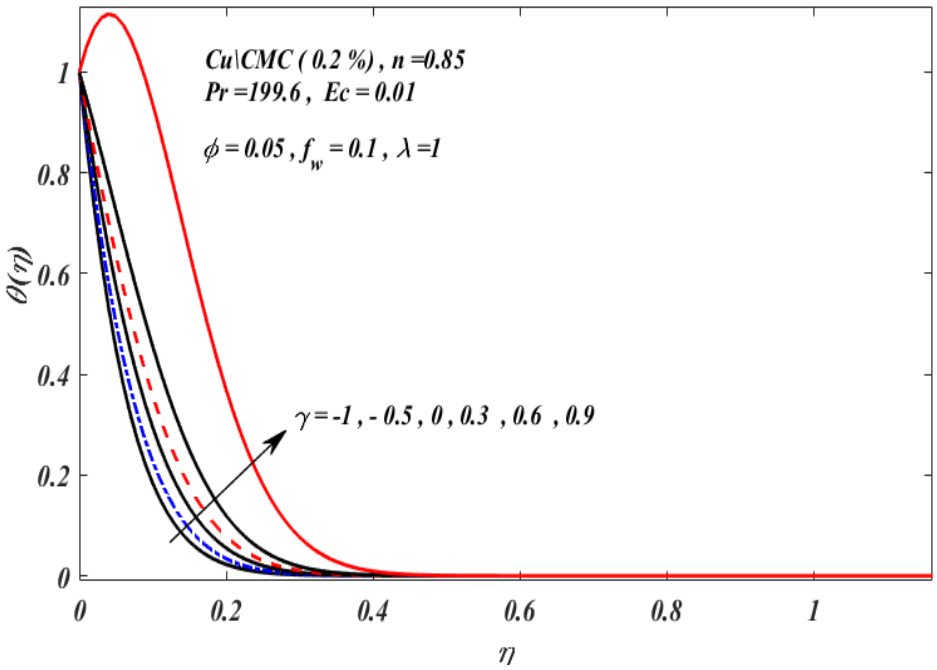

Figure 3.8: Effect of absorption/generation parameter γ on heat profile.

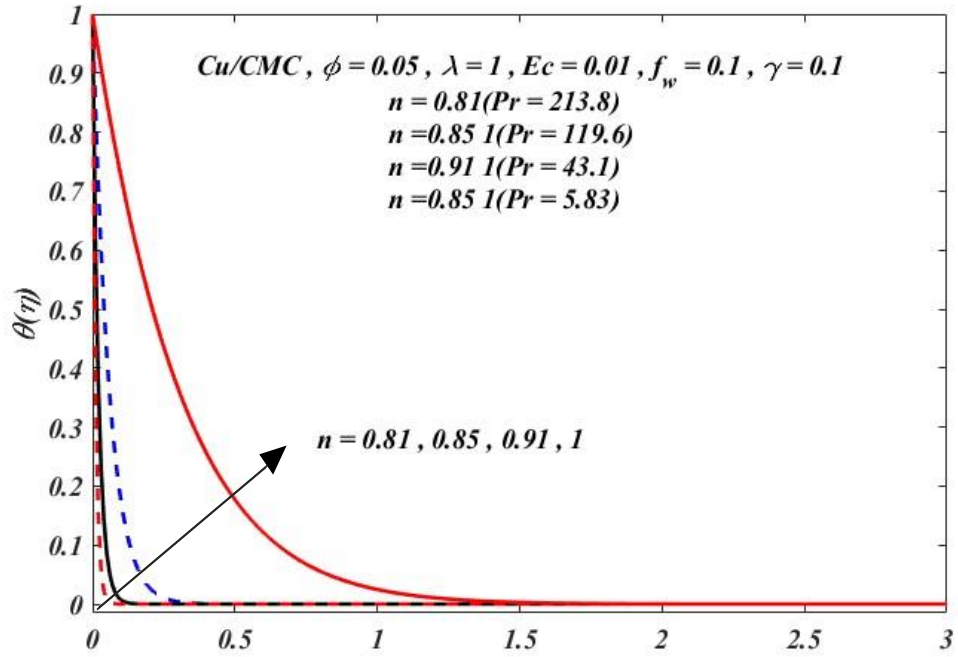

Figure 3.9: Influence of power law index and Prandtl numberPr on $\theta(\eta)$.

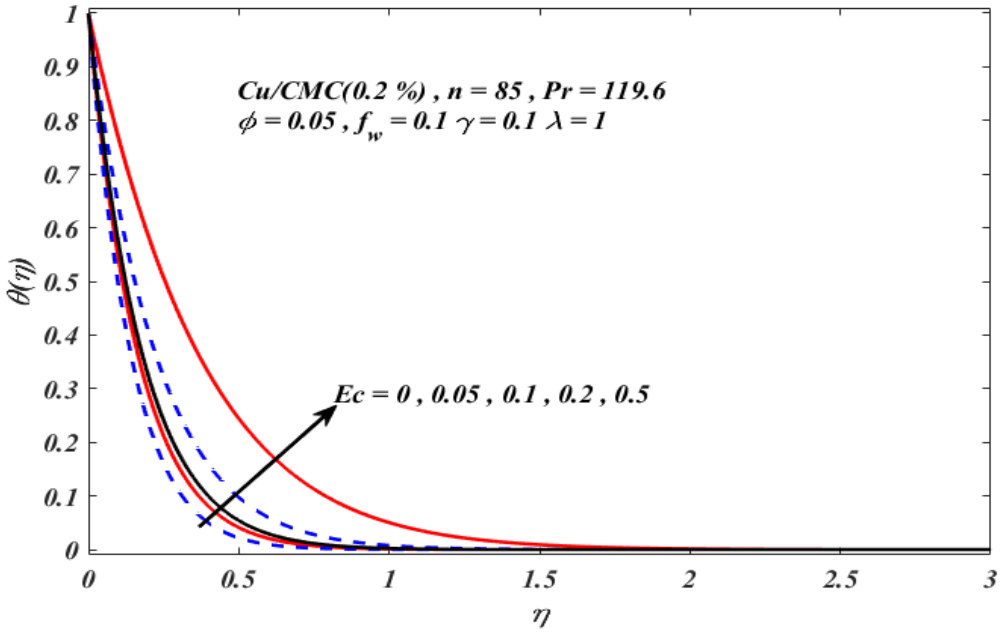

Figure 3.10: Effect of Eckert number (Ec) on temperature profile $\theta(\eta)$.

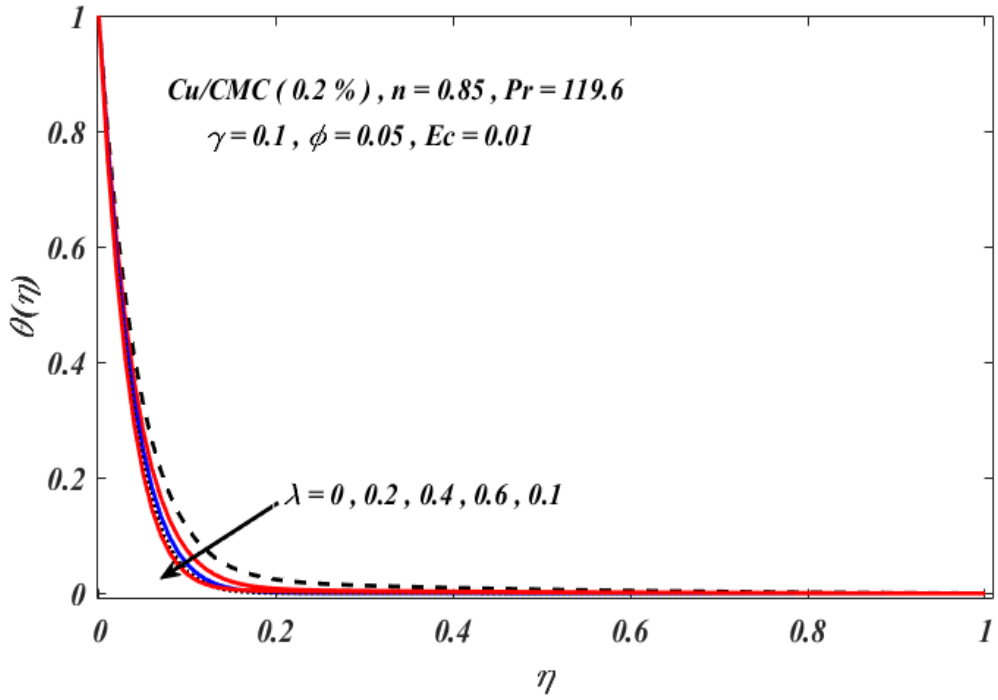

Figure 3.11: Effect velocity ratio λ of temperature profile $\theta(\eta)$.

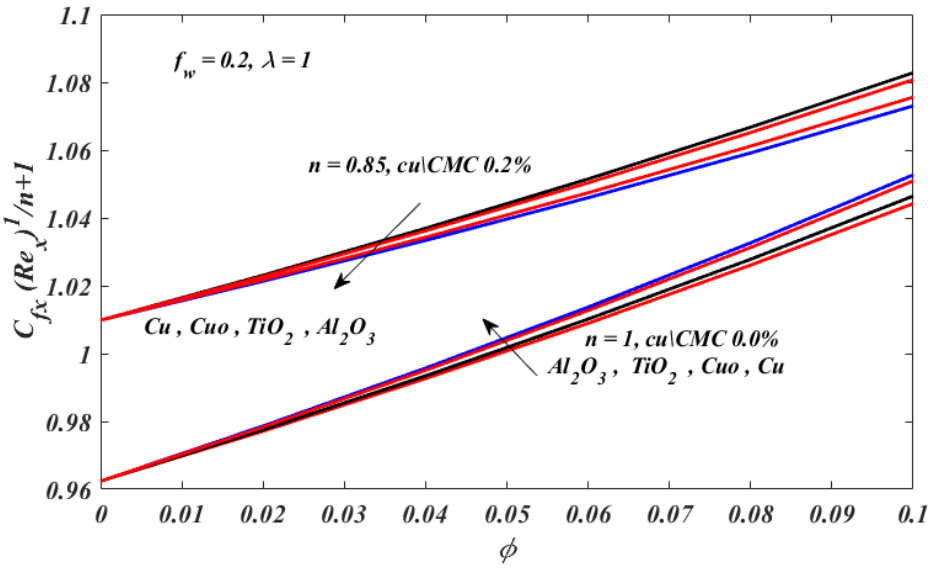

Figure 3.12: Effect of $C_{fx}Re_x^{\frac{-1}{n+1}}$ with nano particle volume fraction of several nanofluids.

Chapter 4

Impact of HH reactions in the flow of pseudo-plastic fluid with MHD and generalized Slip.

4.1 Introduction

This chapter analysis of Pseudo-plastic nanofluid with homogeneous-heterogeneous concentrations having MHD effect and generalized slip condition. The governing PDE are transformed into ODE by using similarity transformations. The nonlinear dimensionless equations are solved numerically by using shooting technique with R-K method. The impact of various parameters on temperature and velocity profile are explained through graphs.

4.2 Description of problems

Considered problem of NN flow under the influence of power law fluid model along a horizontal permeable sheet in the presence of MHD B_o and concentration profile. The homogenous heterogenous reactions are consider in the model of the substance A and B ,mathematically addressed by [10]

We can write expression for homogenous reaction in the existence of constant reaction rate.

$$2B + A \rightarrow 3B, \qquad \text{rate} = K_c^* ab^2,$$

We can write expression for heterogenous reaction in the existence of constant reaction rate.

$$\bar{\bar{A}} + 2\bar{\bar{B}} \rightarrow 3\bar{\bar{B}}, \qquad \text{rate} = K_s^* ab^2,$$

Here a and b are concentration for species A and B while K_c^* and K_s^* represent the constant rate. The problem is observed with generalized slip condition on a moving sheet. Free stream velocity and temperature represent by U_∞ and T_∞ as shown in figure (4.1)

respectively. CMC/H_2o used as base fluid NN Nanofluids. The governing equations for flow model are continuity, momentum and energy equation which are written below.

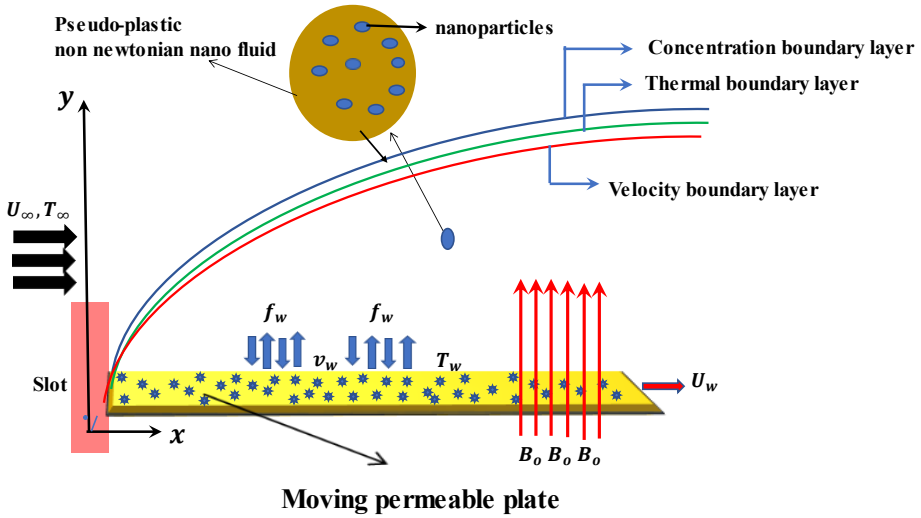

Figure 4.1

4.3 Mathematical analysis

$$\frac{\partial u}{\partial x}+\frac{\partial v}{\partial y}\ =0, \tag{4.1}$$

$$u\frac{\partial u}{\partial x}+v\frac{\partial u}{\partial y}=\ \frac{\mu_{nf}}{\rho_{nf}}\frac{\partial}{\partial y}\left(\left|\frac{\partial u}{\partial y}\right|^{n-1}\frac{\partial u}{\partial y}\right)+\frac{\sigma_{nf}\beta_o}{\rho_{nf}}(u-U_\infty), \tag{4.2}$$

$$\frac{\partial T}{\partial x}+\frac{\partial T}{\partial y}=\alpha_{nf}\frac{\partial^2 x}{\partial y^2}+\frac{\mu_{nf}}{(\rho C_p)_{nf}}\left|\frac{\partial u}{\partial y}\right|^{n+1}+\frac{Q_o(T-T_\infty)}{(\rho C_p)_{nf}}, \tag{4.3}$$

$$u\frac{\partial a}{\partial x}+v\frac{\partial a}{\partial y}=D_A\frac{\partial^2 a}{\partial y^2}-K_c^* ab^2, \tag{4.4}$$

$$u\frac{\partial b}{\partial x}+v\frac{\partial b}{\partial y}=D_B\frac{\partial^2 b}{\partial y^2}+K_c^* ab^2, \tag{4.5}$$

Subject to boundary condition,

$$\left.\begin{aligned} u = U_w + \alpha^* \left[1 - \beta^* \left(\left|\frac{\partial u}{\partial y}\right|^{n-1} \frac{\partial u}{\partial y}\right)\right] \left[\left|\frac{\partial u}{\partial y}\right|^{n-1} \frac{\partial u}{\partial y}\right]^{-\frac{1}{2}}, \\ v = -v_w, \;\; T = T_w, \\ D_A \frac{\partial a}{\partial y} = K_s a, D_B \frac{\partial b}{\partial y} = -K_s a \, , \end{aligned}\right\} \quad at \;\; y = 0, \tag{4.7}$$

$$\left.\begin{aligned} u \to U_\infty, v = -v_w, \; T \to T_\infty, \\ a \to a_0, \;\; b \to 0, \end{aligned}\right\} \quad at \quad y \to \infty. \tag{4.8}$$

Useful similarity variables are given (3.5) and concentration parameters are

$$a = a_o G(\eta) \, , \quad b = a_o H(\eta), \tag{4.9}$$

Using similarity transformation partial differential equations (4.1-4.5) converted into ordinary differential equations in the form

$$m_o(|f''|^{n-1}f'')' - M^2 m_6 m_7 (f' - \lambda) + \tfrac{1}{(n+1)} \; ff'' = 0, \tag{4.9}$$

$$\theta'' + \tfrac{P_r m_1}{(n+1)} f\theta + \;\; P_r m_1 m_2 Ec|f''|^{n+1} + P_r m_1 m_3 \gamma\theta = 0, \tag{4.10}$$

$$\tfrac{1}{Sc} G'' + \tfrac{1}{(n+1)} fG' - KH^2 = 0, \tag{4.11}$$

$$\tfrac{\delta}{Sc} H'' + \tfrac{1}{(n+1)} fH' + KGH^2 = 0, \tag{4.12}$$

Subject to boundary conditions,

$$\left.\begin{aligned} f' = \lambda + \epsilon(1 - \text{ɾ} f''|f''|^{n-1})^{-\frac{1}{2}} f''|f''|^{n-1}), \;\; f = f_w, \;\; \theta = 1, \\ G' = K_s G, \;\; H' = -K_s G\sigma, \end{aligned}\right\} at \;\; \eta = 0, \tag{4.13}$$

$$\left.\begin{aligned} f' \to 1 - \lambda, \quad f = f_w, \;\; \theta \to 0, \\ G \to 1, \;\; H \to 0, \end{aligned}\right\} at \;\; \eta \to \infty. \tag{4.14}$$

where ϵ and ɾ represent the tangential velocity, Navier's slip length and the reciprocal of some critical shear rate.

Some useful parameters are given below

$$\left.\begin{aligned} Sc = \frac{U}{D_A x}\left(\frac{U^{2-n}}{\nu_f x}\right)^{-\frac{2}{n+1}}, \delta = \frac{D_A}{D_B}, M = \frac{x\sigma\beta_o}{U\rho_{nf}} \\ \epsilon = \frac{\alpha U^{2n-1}}{\vartheta_f^{n/n+1} x^{\frac{n}{n+1}}}, \lambda = \frac{\beta(U^3)^{x^{\frac{n}{n+1}}}}{\vartheta_f^{n/n+1} x^{\frac{n}{n+1}}}, \end{aligned}\right\}, \tag{4.15}$$

Engineering quantities.

$$m_6 = \frac{1}{(1-\phi+\phi\left(\frac{\rho_S}{\rho_f}\right)}, \quad m_7 = \frac{1+3\phi\left(\frac{\sigma_S}{\sigma_f}\right)-1}{\left(\frac{\sigma_S}{\sigma_f}+2\right)-\left(\frac{\sigma_S}{\sigma_f}-1\right)\phi}, \tag{4.16}$$

4.4 Results and Discussion

The governing equations are solved numerically with the help of R-K method and represented graphically. Figure (4.2) represents the behavior of suction-injection parameter against velocity profile of nanofluid. Figure (4.2) shows that by increasing suction parameter f_w the velocity profile also increases for both of fluid i.e., pseudo-plastic and dilatant fluid.

Figure (4.3) signifies the conduct of volume fraction on velocity profile. Velocity decreases by inclination of volume fraction parameter ϕ. The figure (4.4) states that impact of velocity ratio against velocity profile. When λ is in the range of 0 to 0.4 flow velocity is greater than plat velocity but when its range is 0.6 to 1 then plate have greater velocity as compared to free flow velocity. Lastly, when λ have value is 0.5 then observed velocity is same for flow and plat velocity and observed to be constant at every point. Figure (4.5) signifies the behavior of generalized slip parameter ϵ against velocity profile $f(\eta)$. Velocity is observed to be decreasing by enlarging the slip parameter ϵ.

Figure (4.6) represents the effect of magnetohydrodynamic parameter on velocity profile. It can notice that by inclining MHD M, the velocity also increases. Figure (4.7) shows the slip parameter λ effect against velocity profile $f'(\eta)$. It is noted that velocity is declining function of slip parameter λ. In figure (4.8), it can be clearly seen that the

behavior of suction injection parameter on temperature profile, the graphical representation shows that enhancement in f_w leads to decrease in temperature.

Figure (4.9) represents the effect of thermal generation/absorption on thermal profile. It is noted that by raising the absorption/generation parameter the temperature inclining. Figure (4.10) shows the characteristics of volume fraction against the temperature profile. The graph represents the temperature increases by increasing the ϕ..In figure (4.11), the effects of power law index (n) and Prandtl number (Pr) are presented for temperature profile $\theta(\eta)$. It is observed that the temperature profile declining by increasing the Pr number.

The figure (4.13) represents the influence of suction injection parameter on concentration profiles $G(\eta), H(\eta)$. Results show that by increasing f_w parameter the concentration $G(\eta)$ rises but $H(\eta)$ is declining. Figure (4.14) specifies the impact of volume fraction on concentration profiles $H(\eta), G(\eta)$. The graph illustrates that by increasing volume fraction parameter ϕ the concentration $G(\eta)$ reduces while the profile $H(\eta)$ increase. Both graphs have opposite behaviors.

Figure (4.15) shows the effect of slip parameter ϵ on concentration $G(\eta), H(\eta)$. The graph reveals that by increasing slip parameter the concentration $G(\eta)$ also decreases. On the other hand, the concentration profile $H(\eta)$ decreases Both graphs have opposite behaviors. Figure (4.16) represents the behavior of slip parameter ɾ against concentration. It can be clearly seen that reducing slip parameter ɾ, the concentration profiles have opposite behaviors. The graph of $G(\eta)$ is increasing while the graph of $H(\eta)$ is decreasing. Figure (4.17) showing effect of Sc on concentration profile, it declares that graphs have opposite behavior for increasing Sc. The graph of $G(\eta)$ increases but $H(\eta)$ is decreasing.

Figure (4.18) denote the effect of strength of homogeneous reaction on concentration profile. Concentration is observed by increasing the strength parameter K. The graph of $G(\eta)$ is decreasing but $H(\eta)$ is increasing Figure (4.19) represents the outcome of strength of heterogeneous reaction on concentration profiles. It is noted that concentration profile having opposite behaviors for parameter K_s. The graph of $G(\eta)$ is increasing while the graph of $H(\eta)$ is decreasing. Figure (4.20) shows the effect of σ on concentration profile.

Concentration profile having opposite behaviors when σ is enhancing. $G(\eta)$ is increasing while $H(\eta)$ is decreasing so both graphs have opposite behaviors. Figure (4.21) is showing the impact of strength of diffusion coefficient δ on concentration. By increment in δ the graph of concentration profile $G(\eta)$ is decreasing but for $H(\eta)$ the graph is increasing.

From figure (4.22) shows that by increasing M the graph of $H(\eta)$ is decreasing but the graph of $G(\eta)$ is increasing. From figure (4.23) it is observed that by increasing ζ the graph of $H(\eta)$ is increasing but the graph of $G(\eta)$ is decreasing. From figure (4.24) by increasing ϵ the graph of $H(\eta)$ is increasing but the graph of $G(\eta)$ is decreasing. It can be seen from figure (4.25), drag friction coefficient is increased by enhancement of volume fraction ϕ for Newtonian as well as pseudo-plastic non-Newtonian liquid. From figure values of skin friction factor highest or lowest depend on Cu and Al_2O_3 based nanofluids, correspondingly.

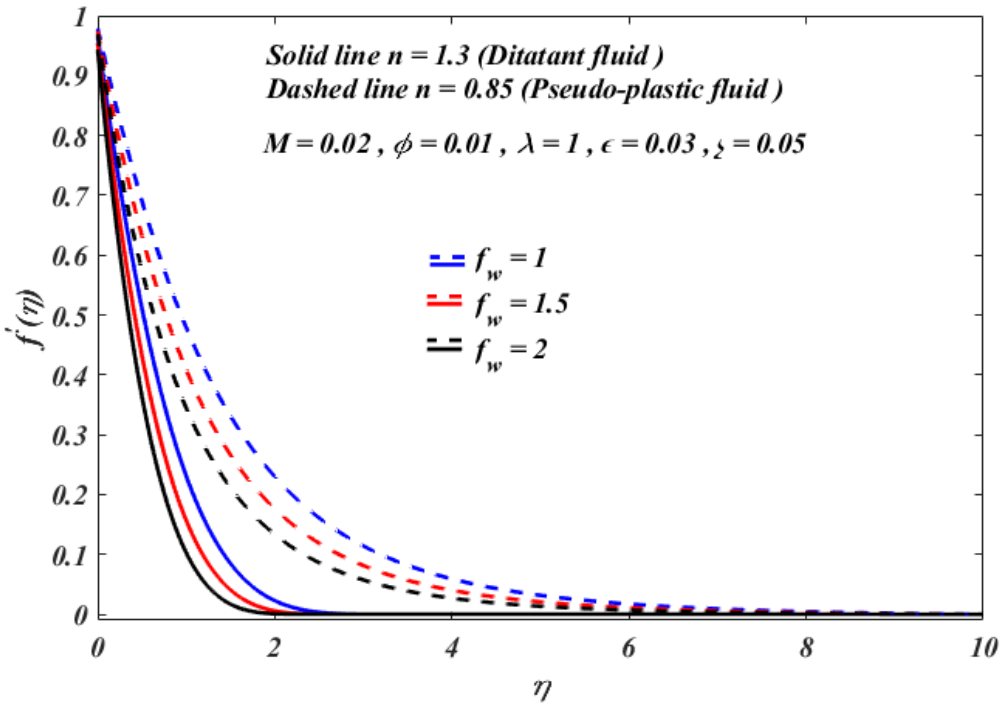

Figure 4.2: Effect of permeable suction f_w parameter on $f'(\eta)$.

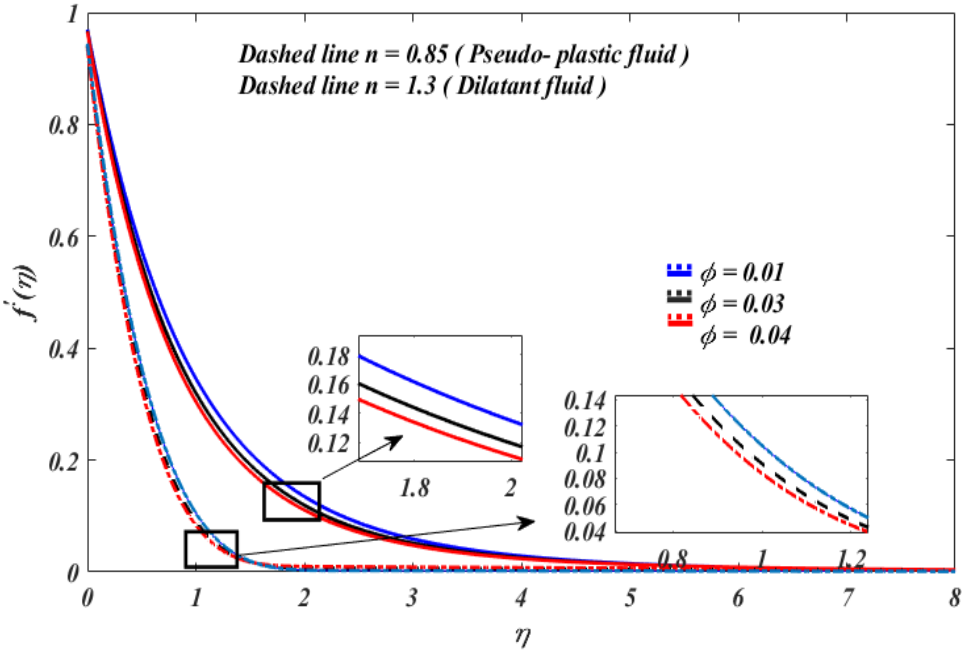

Figure 4.3: Effect of volume fraction parameter ϕ on $f'(\eta)$.

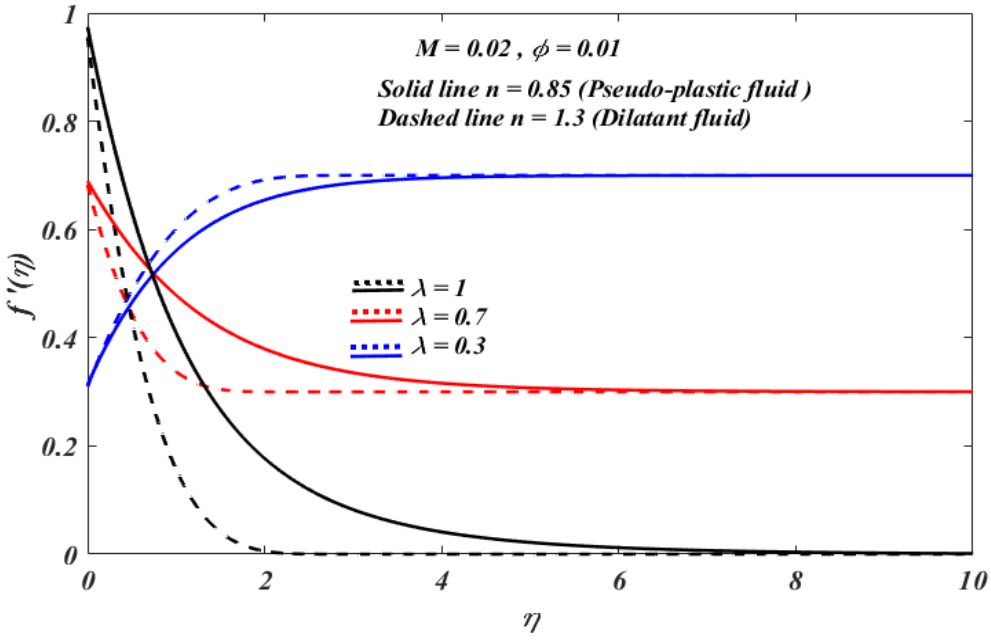

Figure 4.4: Effect of velocity ratio λ on velocity profile $f'(\eta)$.

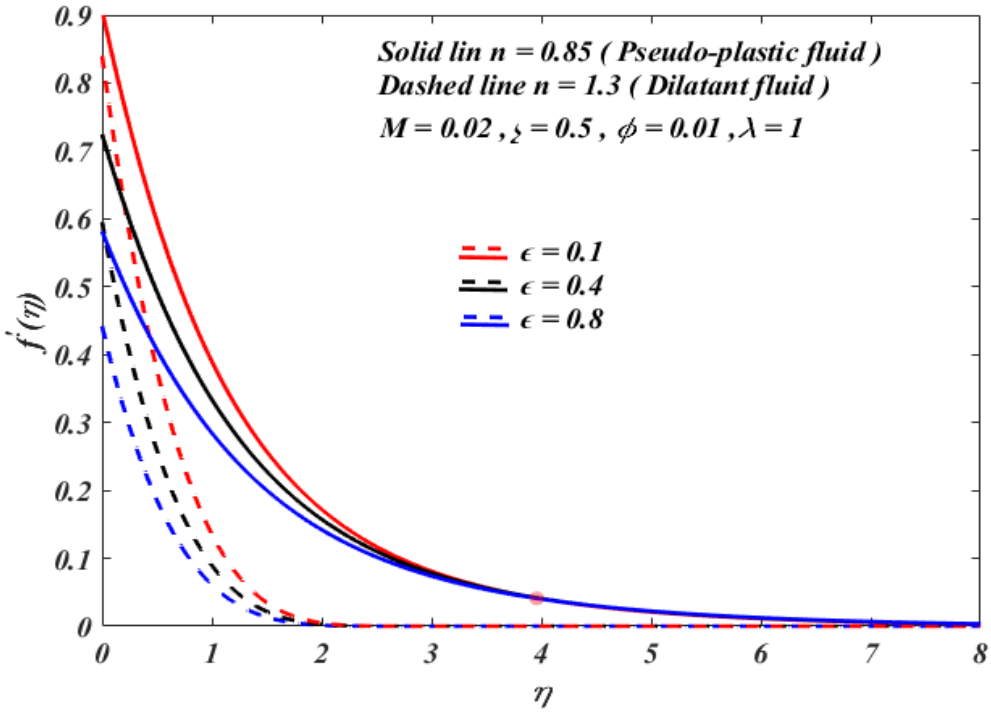

Figure 4.5: Effect of generalized slip parameter ϵ on velocity profile $f'(\eta)$.

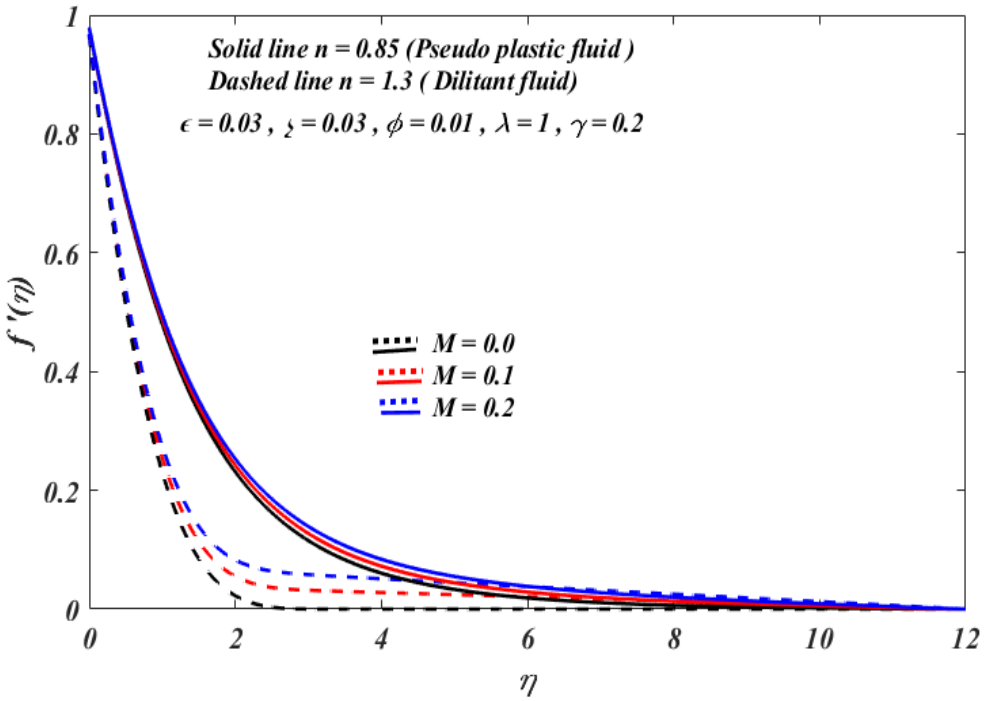

Figure 4.6: Effect of MHD parameter M on velocity profile $f'(\eta)$.

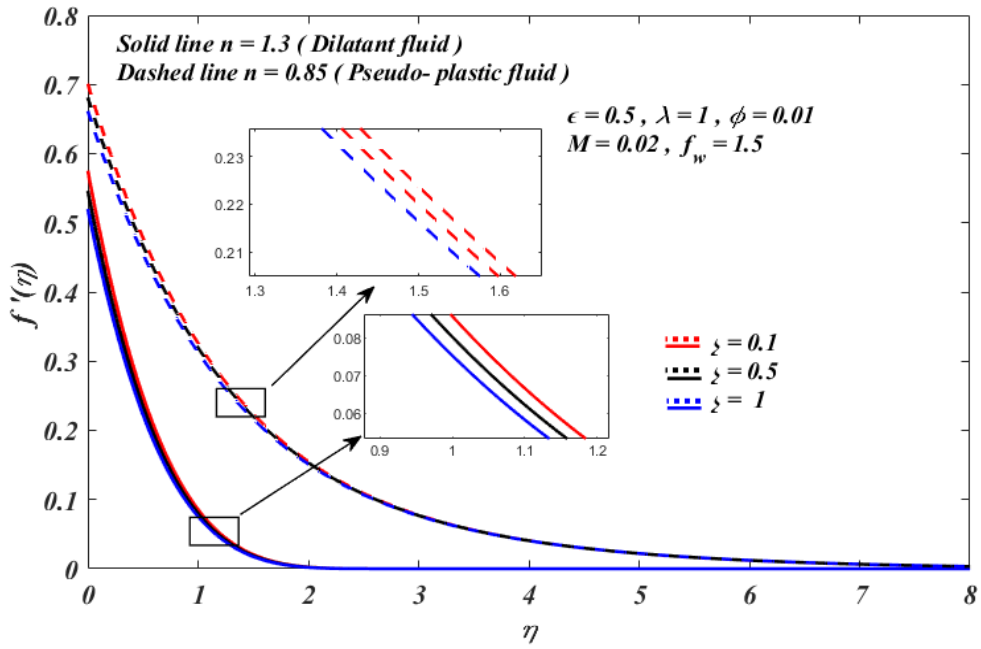

Figure 4.7: Effect of slip parameter $\wr$ on velocity profile $f'(\eta)$.

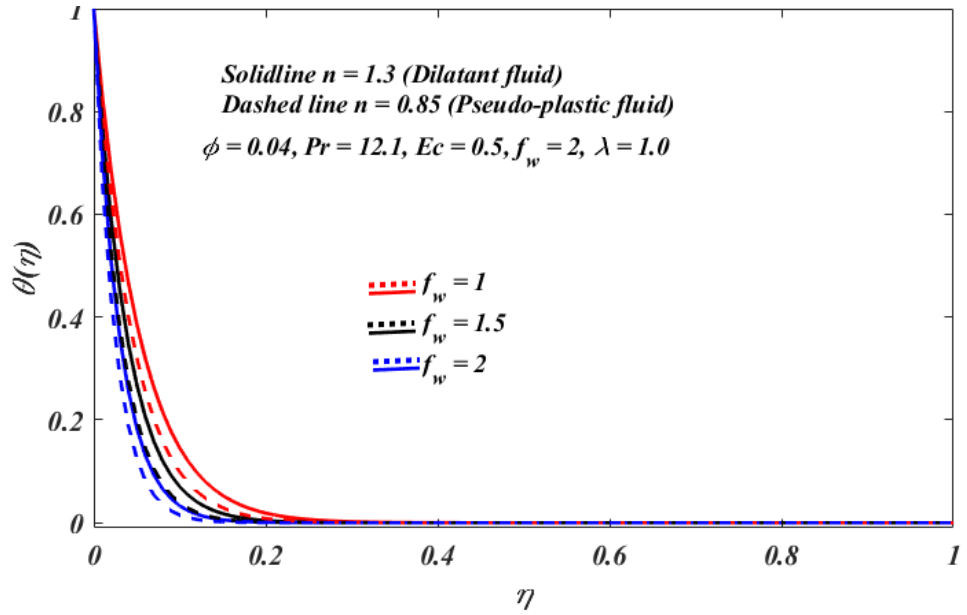

Figure 4.8: Effect of suction parameter f_w on temperature profile $\theta(\eta)$.

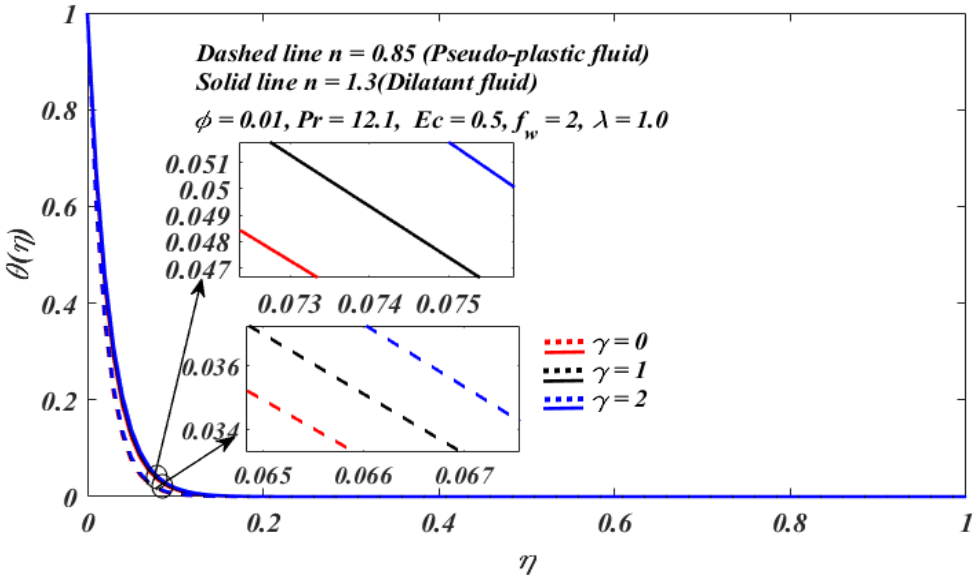

Figure 4.9: Effect of thermal absorption/generation parameter γ against $\theta(\eta)$.

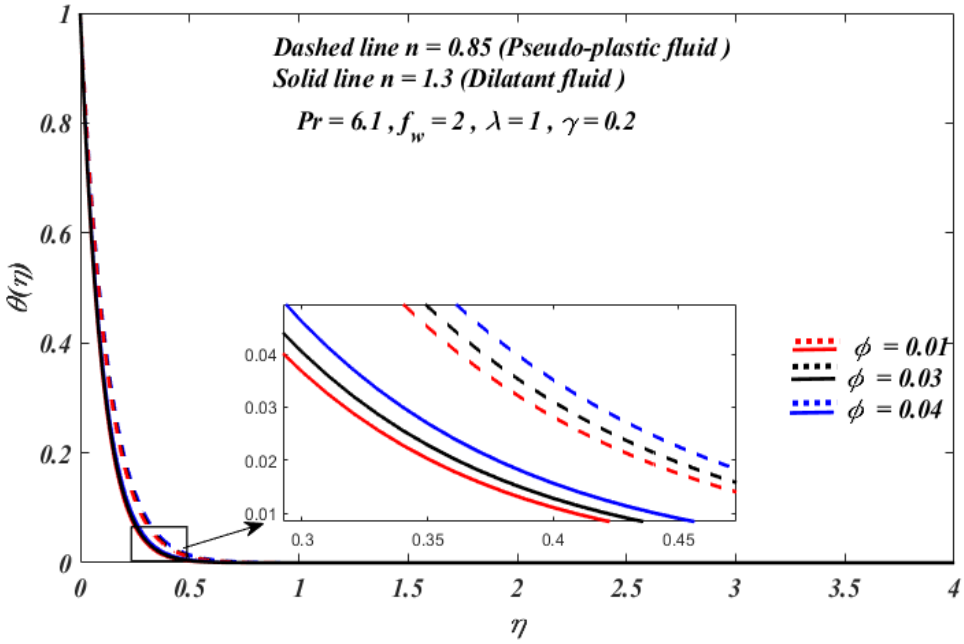

Figure 4.10: Effect of volume fraction parameter (ϕ) on temperature profile $\theta(\eta)$.

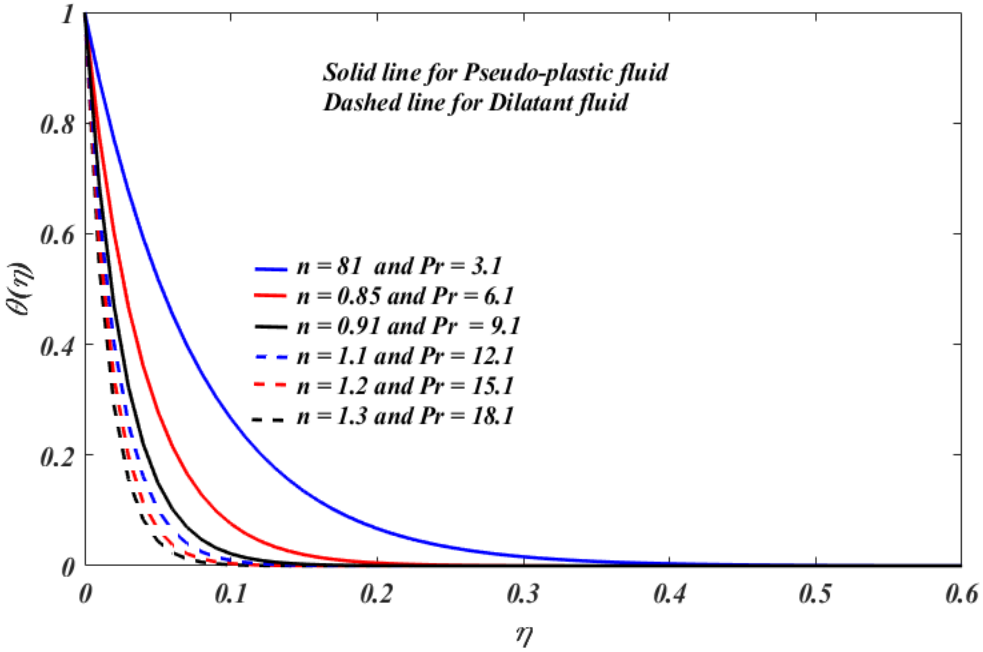

Figure 4.11: Effect of PLI (n) and Prandtl number on temperature profile $\theta(\eta)$.

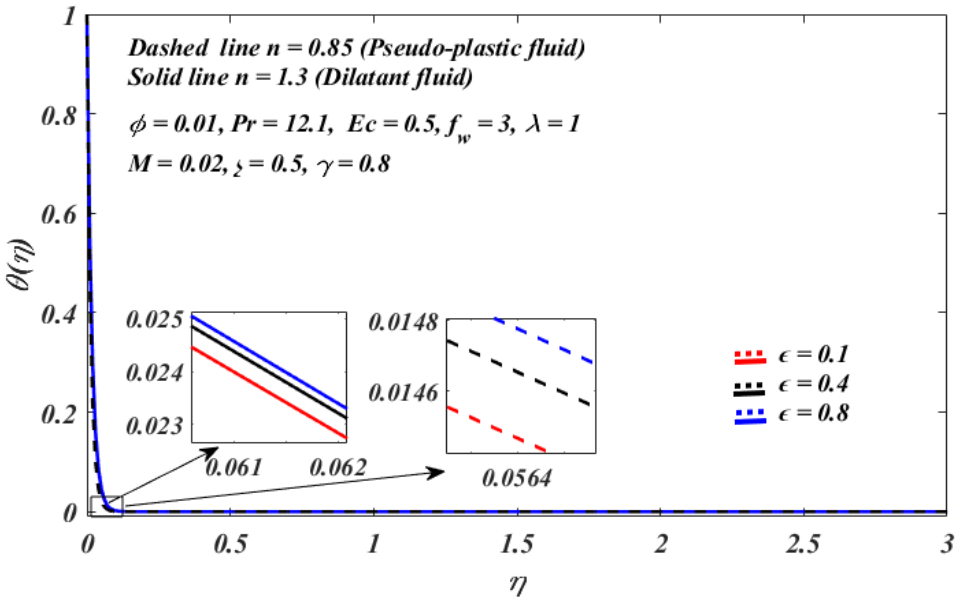

Figure 4.12: Effect of ϵ slip parameter on temperature profile $\theta(\eta)$.

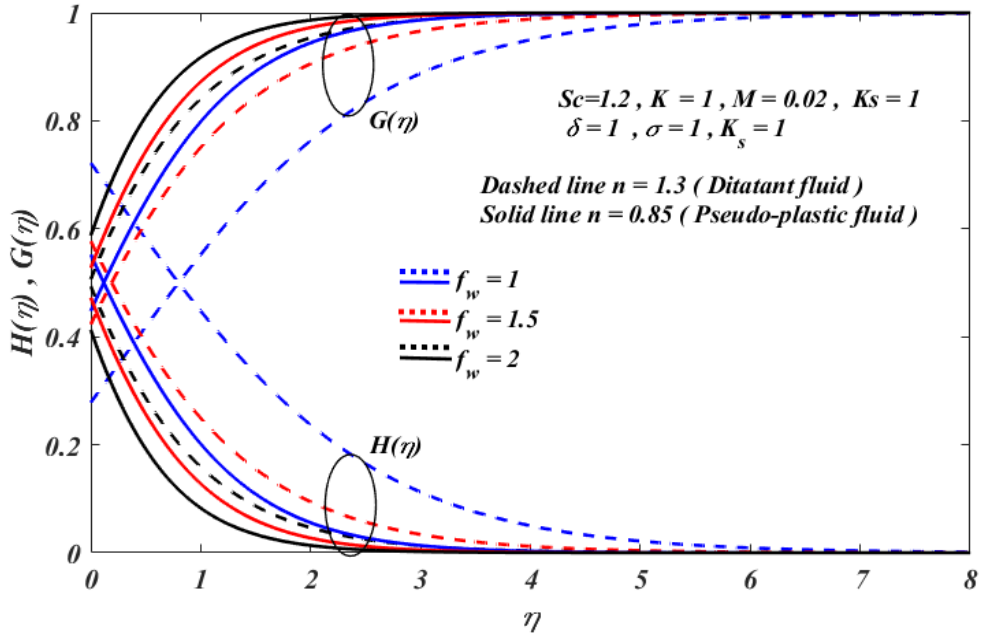

Figure 4.13: Effect of f_w on concentration profile $G(\eta), H(\eta)$.

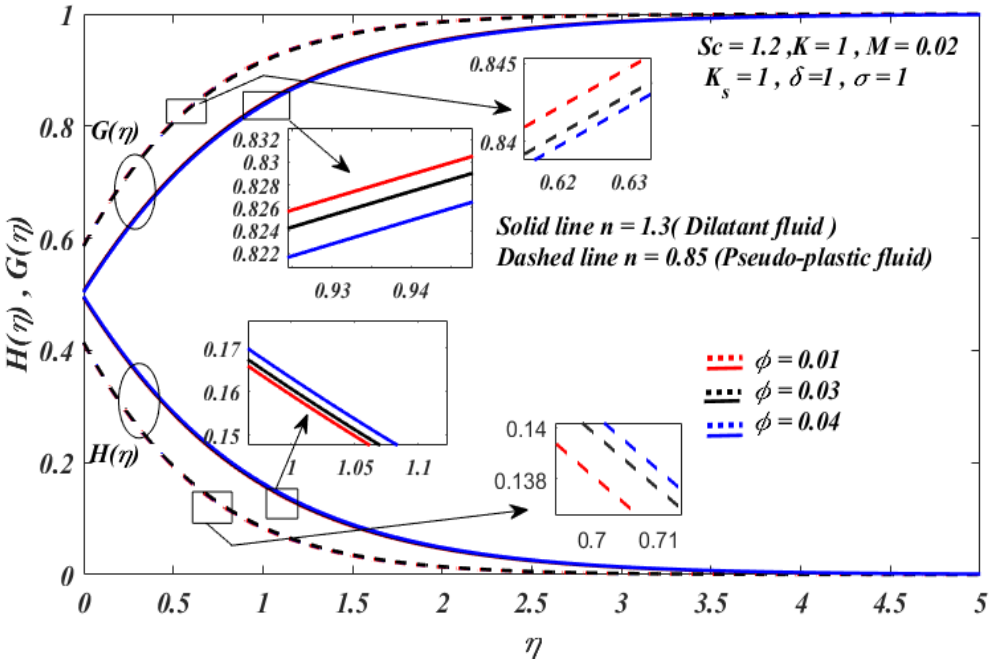

Figure 4.14: Effect of ϕ on concentration profile $H(\eta), G(\eta)$.

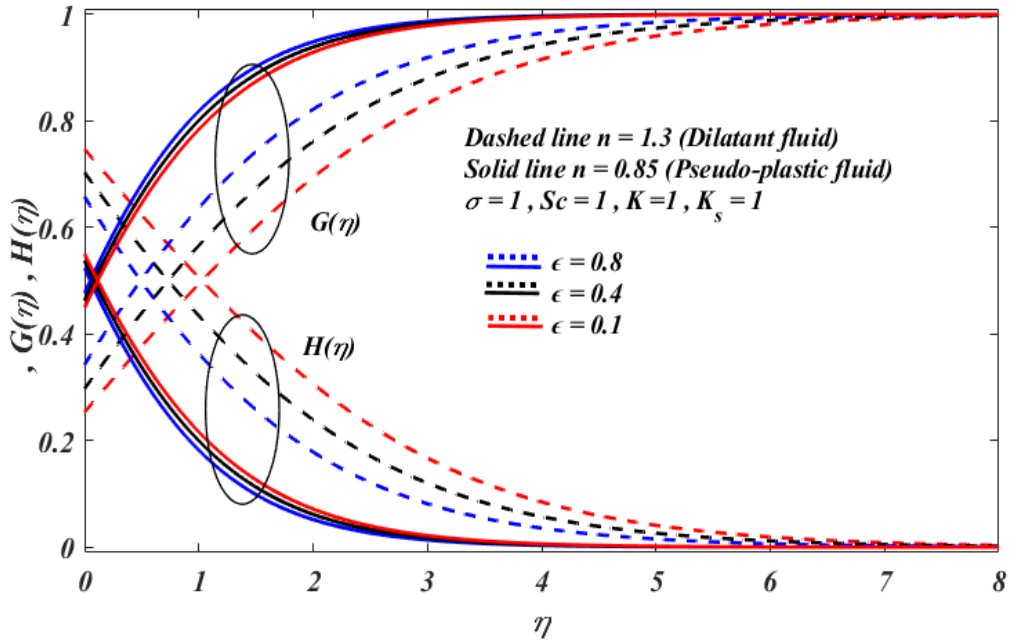

Figure 4.15: Effect of ϵ parameter on concertation profile $G(\eta), H(\eta)$.

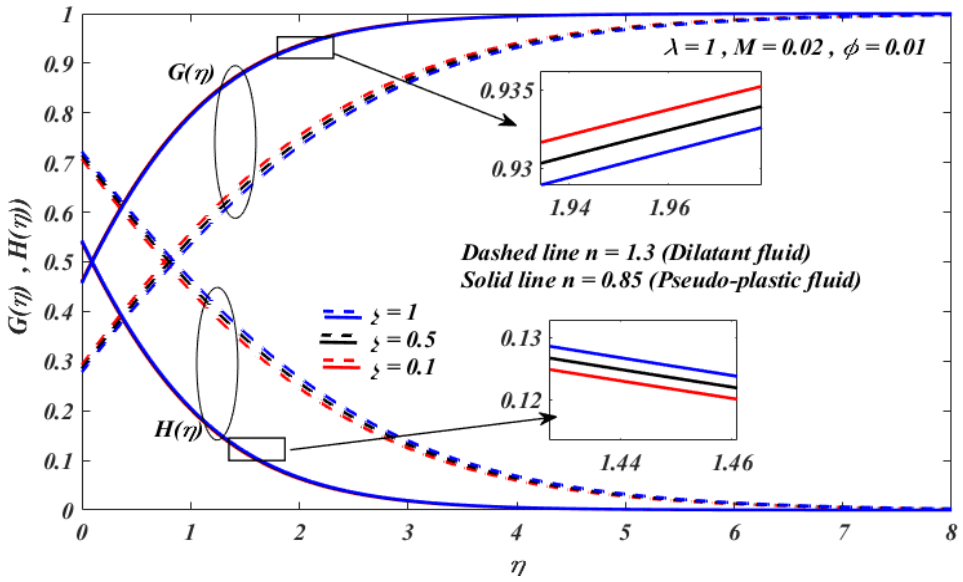

Figure 4.16: Effect of $\wr$ slip parameter on concentration profile $G(\eta), H(\eta)$.

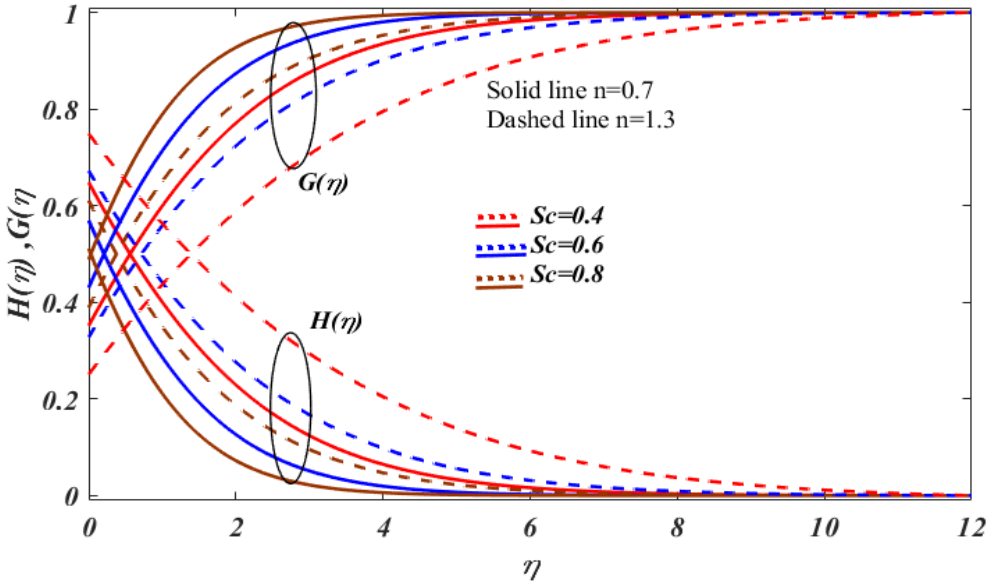

Figure 4.17: Effect of Sc on concentration profile $G(\eta), H(\eta)$.

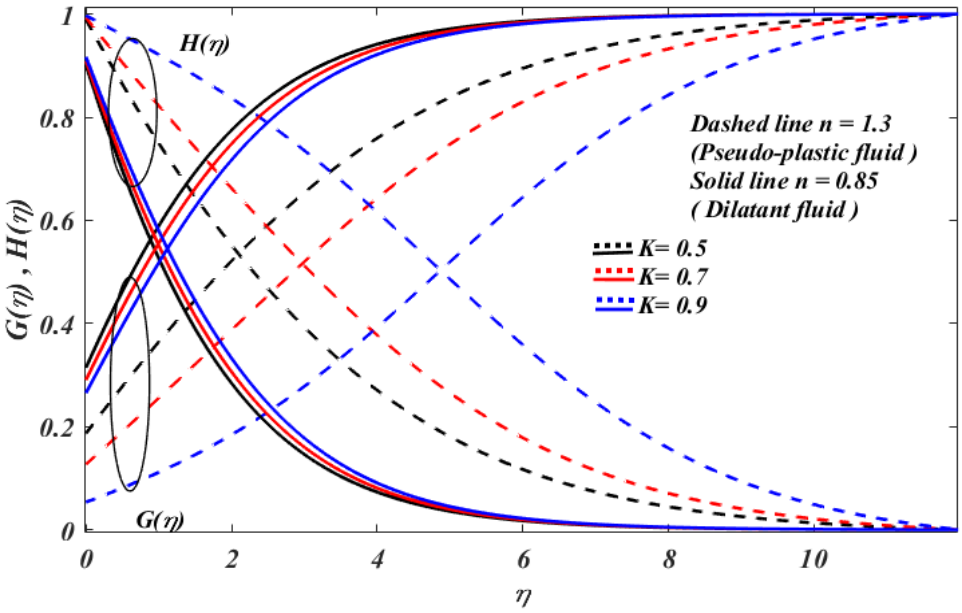

Figure 4.18: Effect of strength of homogeneous reaction K on concentration profile $G(\eta), H(\eta)$.

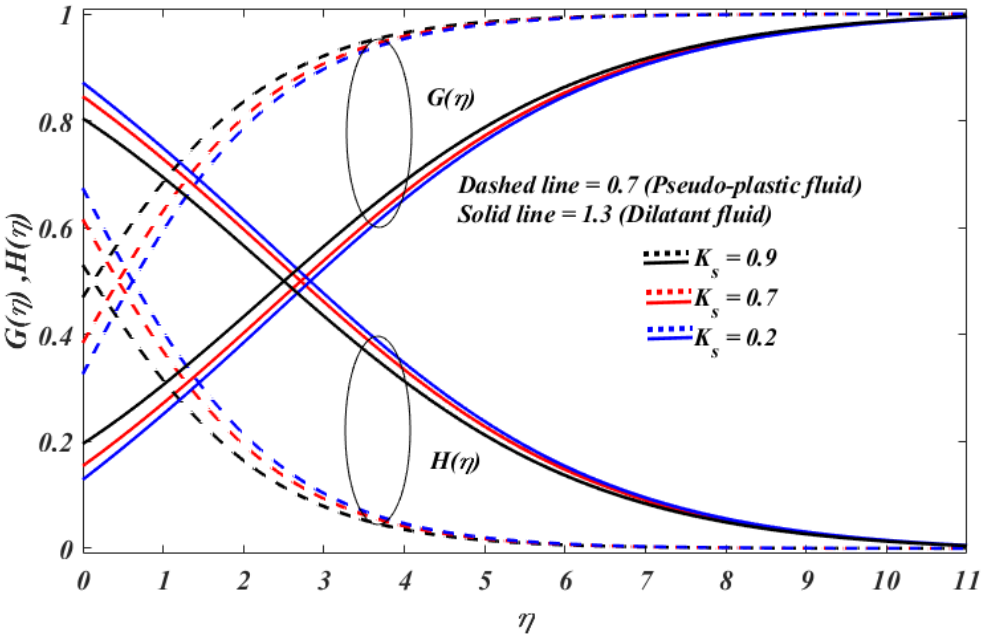

Figure 4.19: Effect of strength of heterogeneous reaction K_s on concentration profile $G(\eta), H(\eta)$.

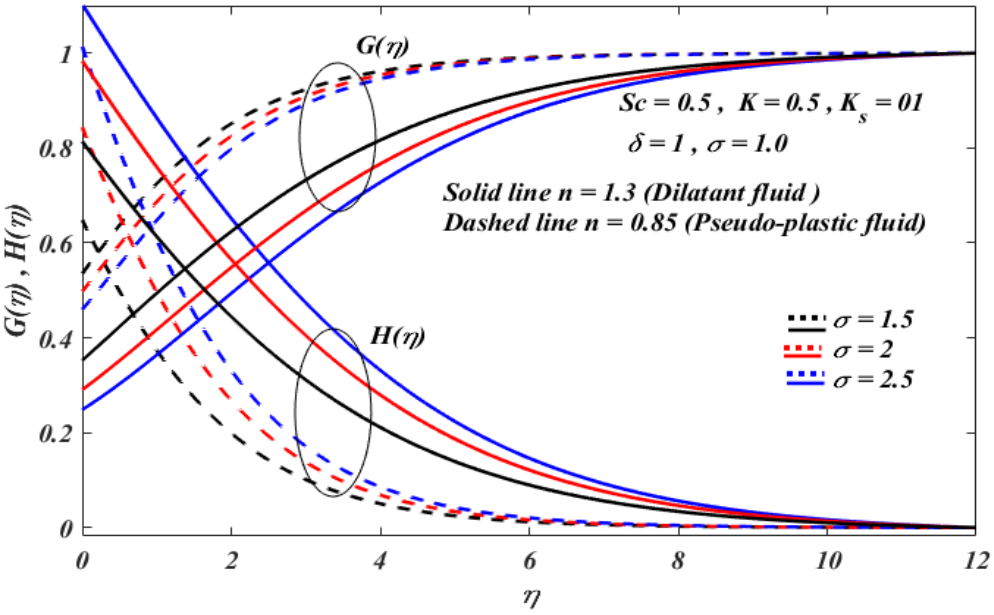

Figure 4.20: Diffusion of heterogeneous reaction σ on concentration profile $G(\eta), H(\eta)$.

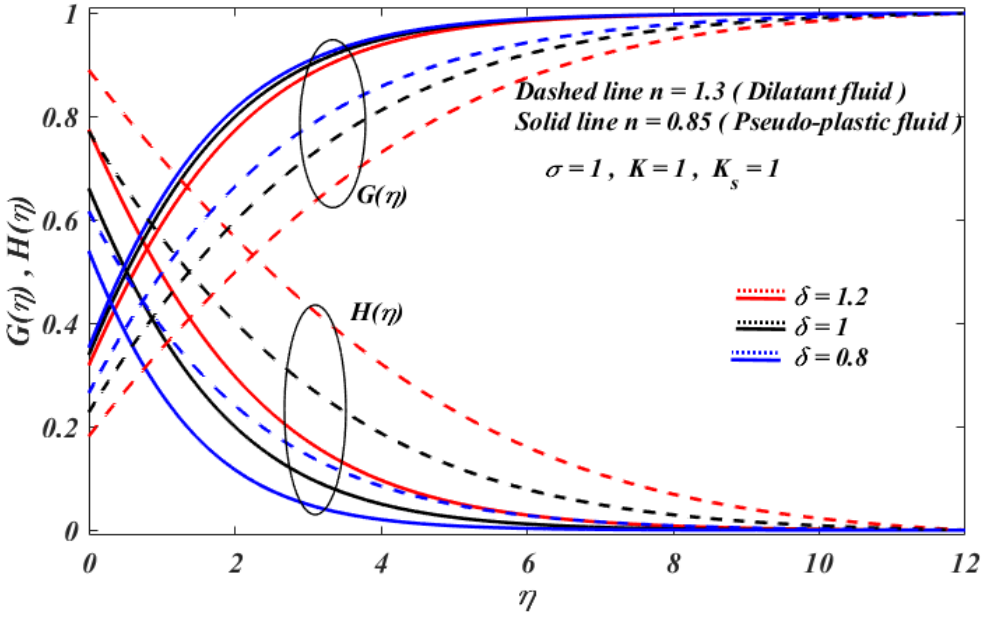

Figure 4.21: Effect of δ on concentration profile $G(\eta), H(\eta)$.

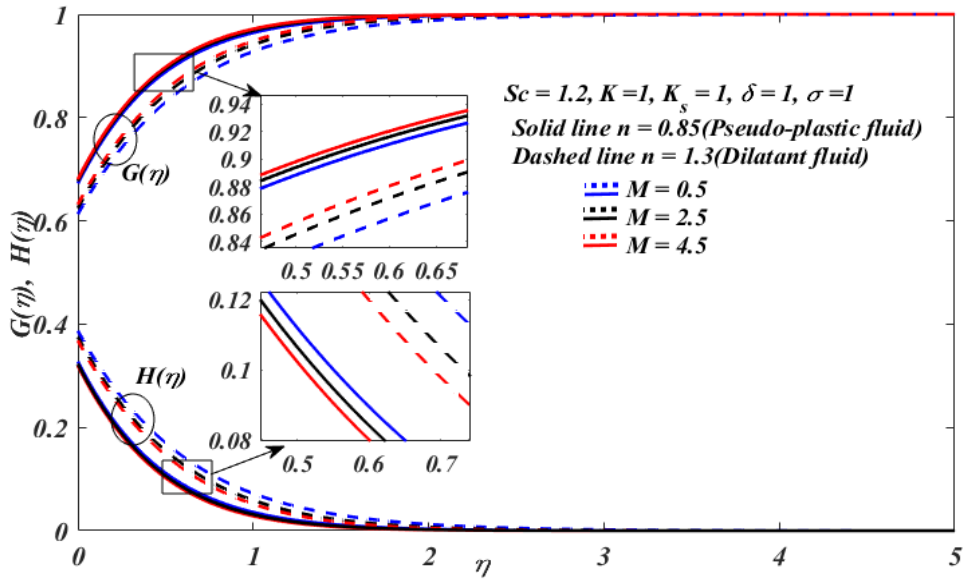

Figure 4.22: Effect of MHD (M) on concentration profile $G(\eta), H(\eta)$.

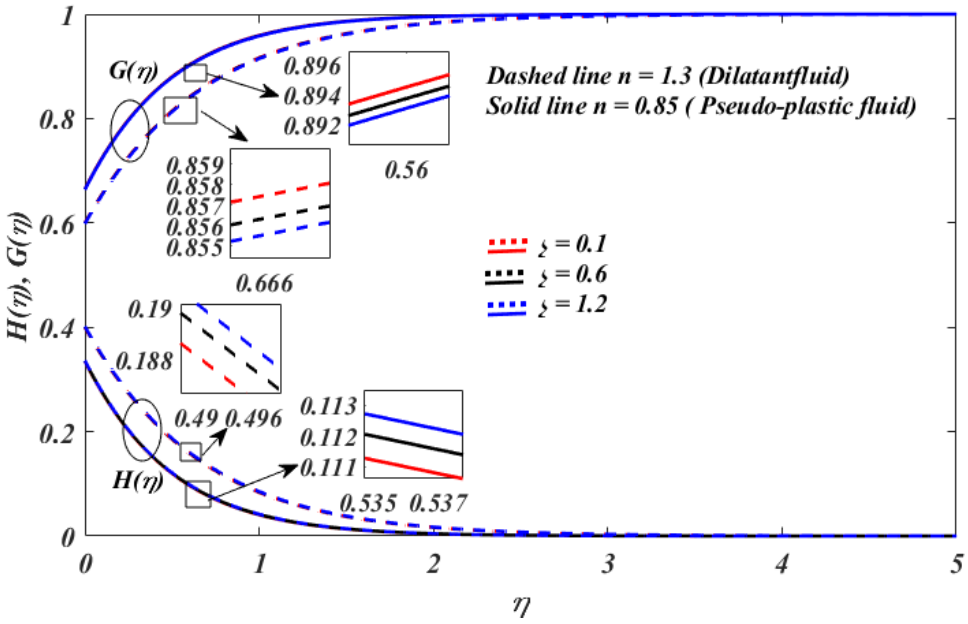

Figure 4.23: Effect of $\wr$ on concentration profile $G(\eta), H(\eta)$.

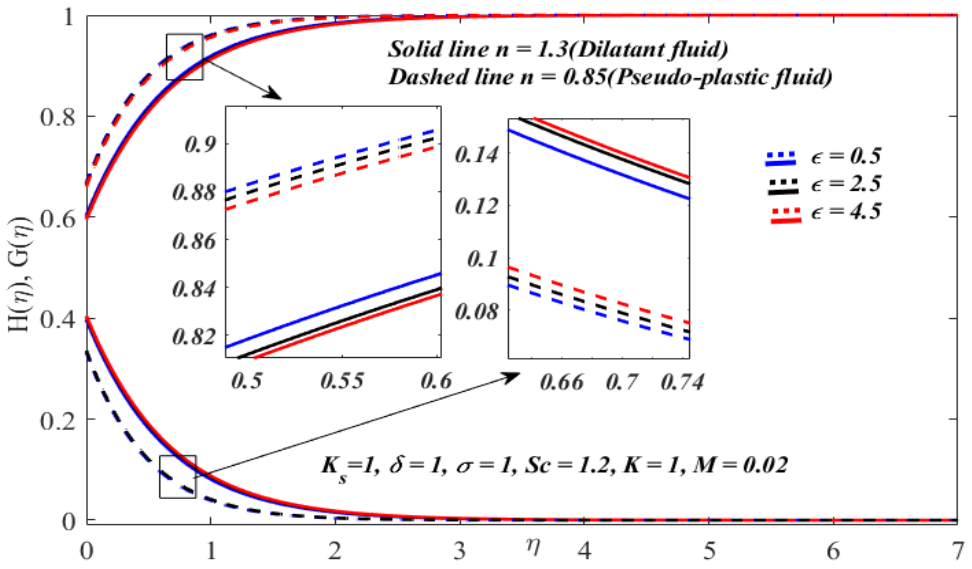

Figure 4.24: Effect of ϵ on concentration profile $G(\eta), H(\eta)$.

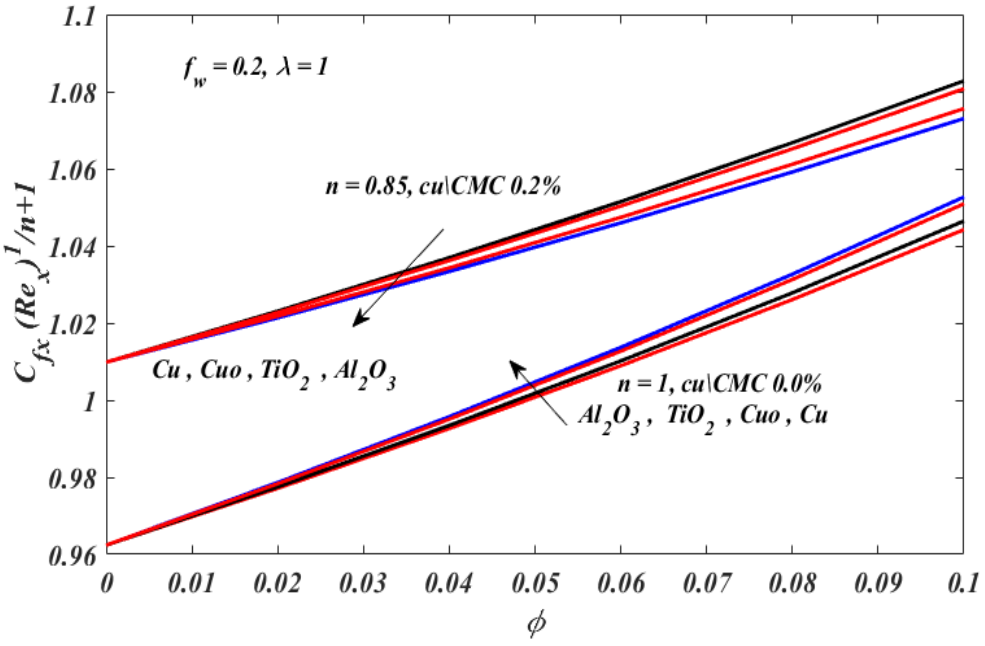

Figure 4.25: Effect of $C_{fx}Re_x^{\frac{-1}{n+1}}$ with nano particle volume fraction of several nanofluids.

Chapter 5

Conclusion

This chapter consists of concluding remarks of all previous chapters. It is the analysis of HH reactions in the flow of Pseudo-plastic nanofluid with the existence of MHD past a spongy stretching sheet. Furthermore, generalized slip condition is also considered. By using similarity variables, the governing PDEs are converted into ODE. Constructed problem is solved numerically by employing shooting technique and R-K method with the help of mathematical software MATLAB.

Final remarks

The chapter 4 is the extension work of chapter 3 which includes the homogeneous heterogeneous reactions in the existence of MHD and generalized slip boundary condition. The conclusion of chapter 4 is summarized as

- The velocity and temperature profiles increase with enhancement in Suction/injection f_w.
- The homogeneous reaction profile increases when f_w is increased while heterogeneous reaction profile is decreased with increase in f_w.
- The velocity and temperature profiles are increasing functions of generalized slip condition.
- Increment in MHD cause an increase in the velocity profile.
- Graph of temperature profile is increasing with decrease in Prandtl number.
- It is observed that by inclining volume fraction ϕ , the heat and velocity profiles are reduced.
- The homogeneous reaction profile increases with an augment in Sc while heterogeneous reaction decreases.

References

1. Maleki, H., Mohammad Reza Safaei Hussein Togun Mahidzal Dahari5., Heat transfer and fluid flow of pseudo-plastic nanofluid over a moving permeable plate with viscous dissipation and heat absorption/generation. Journal of Thermal Analysis and Calorimetry, 2018. 135(3): p. 1643-1654
2. Kardgar, A., Numerical investigation of MHD oscillating power-law non-Newtonian nanofluid flow in an enclosure. The European Physical Journal Plus, 2021. 136(1).
3. Javaid, S., A. Aziz, and A.M.B. Pereira, Group Invariant Solutions for Flow and Heat Transfer of Power-Law Nanofluid in a Porous Medium. Mathematical Problems in Engineering, 2021. 2021: p. 1-14.
4. Ali, A., R.N. Jana, and S. Das, Hall effects on radiated magneto-power-law fluid flow over a stretching surface with power-law velocity slip effect. Multidiscipline Modeling in Materials and Structures, 2020. 17(1): p. 103-125.
5. Raju, D.G.S.H.S.N.N.K.C.S.K., The impact of thermal stratification and heat generation/absorption on MHD carreau nano fluid flow over a permeable cylinder. Springer Nature Switzerland AG 2020, p. 1-10.
6. Khan, Shahid Khan , Mahmoud M. Selim , Aziz Khan , Asad Ullah , Thabet Abdeljawad , Ikramullah , Muhammad Ayaz and Wali Khan Mashwani On the Analysis of the Non-Newtonian Fluid Flow Past a Stretching/Shrinking Permeable Surface with Heat and Mass Transfer.
7. Khan, I. and A. Alqahtani, MHD Nanofluids in a Permeable Channel with Porosity. Symmetry, 2019. 11(3).
8. Hayat, M.W.A.K.M.W.M.I.K.A.A.T., MHD stagnation point flow accounting variable thickness and slip conditions. Springer-Verlag Berlin Heidelberg 2017 :p. 1-9.
9. Asad Ejaz , I.A., Yasir Nawaz Wasfi Shatanawi , Muhammad Shoaib Arif and Javeria Nawaz Abbasi, Thermal Analysis of MHD Non-Newtonian Nanofluids over a Porous Media. 2020.

10. K. Jabeen , M. Mushtaq, and R. M. Akram Analysis of the MHD Boundary Layer Flow over a Nonlinear Stretching Sheet in a Porous Medium Using Semianalytical Approaches. Hindawi, 2020., p. 1-9.
11. Khan, S.R.R.A.S.M.I.A., Mixed convection MHD flows of Ag, Cu, TiO2 and Al2O3 nanofluids over in unsteady stretching sheet in the presence of heat generation along with radiation\absorption effects. Applied Nanoscience, 2020: p. 1-17.
12. Jagadeeshwar, D.S.a.P., MHD Flow with Hall current and Joule Heating Effects over an Exponentially Stretching Sheet. de guyter, January 14, 2017.
13. Masood Khan, L.A., and Muhammad Ayaz, Numerical simulation of unsteady 3D magneto-Sisko fluid flow with nonlinear thermal radiation and homogeneous–heterogeneous chemical reactions. 2018: p. 1-11.
14. Ibrahim M. Alarifi 1 , A.G.A., 3, M. Osman 1,4, Liaquat Ali Lund 5, and Mossaad Ben Ayed 6, Hafedh Belmabrouk 8,9 and Iskander Tlili 1,*, MHD Flow and Heat Transfer over Vertical Stretching Sheet with Heat Sink or Source Effect. symmetry. 2019.
15. Abbas, Z, M Sheikh , J Hasnain , H Ayaz and A Nadeem., Numerical aspects of Thomson and Troian boundary conditions in *a* Tiwari–Das nanofluid model with homogeneous–heterogeneous reactions. Physica Scripta, 2019. 94(11).Homogeneous-heterogeneous reactions in Williamson fluid model over a stretching cylinder by using Keller box method. 2015.
16. J. Prathap Kumar, J.C.U.a.S.M., Effect of homogeneous and heterogeneous reactions on the solute dispersion in composite porous medium. International Journal of Engineering, Science and Technology Vol. 4, No. 2, 2012, pp. 58-76, 2012.
17. Tasawar Hayat, Z.H., Taseer Muhammad, Ahmed Alsaedi, Effects of homogeneous and heterogeneous reactions in flow of nanofluids over a nonlinear stretching surface with variable surface thickness. Journal of Molecular Liquids, 2016: p. 1-18.

18. Abbas, Z., M Sheikh , J Hasnain, Numerical aspects of Thomson and Troian boundary conditions in a Tiwari–Das nanofluid model with homogeneous–heterogeneous reactions. Physica Scripta, 2019. 94(11).
19. Kameswaran, P.K., a , S. Shaw a , P. Sibanda a, , P.V.S.N. Murthy, Homogeneous–heterogeneous reactions in a nanofluid flow due to a porous stretching sheet. International Journal of Heat and Mass Transfer, 2013. **57**(2): p. 465-472.
20. Khan, M.I., A comparative study of Casson fluid with homogeneous-heterogeneous reactions. J Colloid Interface Sci, 2017. 498: p. 85-90.
21. Kumar, J.P., J.C. Umavathi, and S. Madhavarao, Effect of homogeneous and heterogeneous reactions on the solute dispersion in composite porous medium. International Journal of Engineering, Science and Technology, 2018. 4(2): p. 58-76.
22. Waini, I., A. Ishak, and I. Pop, Hybrid Nanofluid Flow with Homogeneous-Heterogeneous Reactions. Computers, Materials & Continua, 2021. 68(3): p. 3255-3269.
23. Afzal, N, B.A., Elgarvi AA., Momentum and heat transport on a continuous flat surface moving in a parallel stream. Int J Heat Mass Transf, 1993: p.;36:3399–403.
24. H., Z., *A* study of the boundary layer on a continuous moving surface in power law fluids. 2008: p. 1-15.
25. E., A.-N., Application of nanofluids for heat transfer enhancement of separated flows encountered in a backward facing step. Int J Heat Fluid Flow.2008: p.;29:242–9.